Microbiota regulate the ability of lung dendritic cells to induce IgA class-switch recombination and generate protective gastrointestinal immune responses

Darren Ruane,[1,2] Alejo Chorny,[2] Haekyung Lee,[1,2] Jeremiah Faith,[2] Gaurav Pandey,[3] Meimei Shan,[2] Noa Simchoni,[2] Adeeb Rahman,[2] Aakash Garg,[1] Erica G. Weinstein,[2] Michael Oropallo,[2] Michelle Gaylord,[1,2] Ryan Ungaro,[1] Charlotte Cunningham-Rundles,[2] Konstantina Alexandropoulos,[2] Daniel Mucida,[4] Miriam Merad,[2] Andrea Cerutti,[2] and Saurabh Mehandru[1,2]

[1]Division of Gastroenterology, Department of Medicine, [2]The Immunology Institute, and [3]Department of Genetics and Genomic Sciences and Icahn Institute for Genomics and Multiscale Biology, Icahn School of Medicine at Mount Sinai, New York, NY 10029
[4]Laboratory of Mucosal Immunology, The Rockefeller University, New York, NY 10065

Protective immunoglobulin A (IgA) responses to oral antigens are usually orchestrated by gut dendritic cells (DCs). Here, we show that lung CD103$^+$ and CD24$^+$CD11b$^+$ DCs induced IgA class-switch recombination (CSR) by activating B cells through T cell–dependent or –independent pathways. Compared with lung DCs (LDC), lung CD64$^+$ macrophages had decreased expression of B cell activation genes and induced significantly less IgA production. Microbial stimuli, acting through Toll-like receptors, induced transforming growth factor-β (TGF-β) production by LDCs and exerted a profound influence on LDC-mediated IgA CSR. After intranasal immunization with inactive cholera toxin (CT), LDCs stimulated retinoic acid–dependent up-regulation of α4β7 and CCR9 gut-homing receptors on local IgA-expressing B cells. Migration of these B cells to the gut resulted in IgA-mediated protection against an oral challenge with active CT. However, in germ-free mice, the levels of LDC-induced, CT-specific IgA in the gut are significantly reduced. Herein, we demonstrate an unexpected role of the microbiota in modulating the protective efficacy of intranasal vaccination through their effect on the IgA class-switching function of LDCs.

IgA, the predominant antibody at mucosal surfaces, is of critical importance to mucosal homeostasis. IgA affects noninflammatory (Cerutti, 2008) sequestration of luminal microbes (Macpherson and Uhr, 2004) and neutralization of toxins (Mazanec et al., 1993). Additionally, IgA is associated with down-regulation of proinflammatory epitopes on commensal bacteria (Peterson et al., 2007), secretion of a biofilm that favors the growth of commensals (Bollinger et al., 2006), direction of luminal bacteria to M cells (Mantis et al., 2002; Favre et al., 2005), maturation of DCs (Geissmann et al., 2001), production of IL-10 (Pilette et al., 2010), and FcαRI-mediated suppression of immune responses (Phalipon and Corthésy, 2003). Through these pleiotropic effects, IgA induces a tolerizing phenotype at mucosal surfaces.

The generation of IgA occurs through class-switch recombination (CSR) of the Ig heavy (IgH) chains. After emigration of naive B cells expressing surface IgM and IgD molecules from the bone marrow (Schlissel, 2003), further development of B cells occurs in germinal centers of secondary lymphoid tissue through somatic hypermutation and CSR (Jacob et al., 1991; Liu et al., 1996). CSR replaces the IgH chain constant region (CH) gene without changing the antigenic specificity, resulting in switch of the Ig isotype from IgM or IgD to either IgG, IgE, or IgA (Chaudhuri and Alt, 2004). IgA class switching can occur in both T cell–dependent (TD) and –independent (TI) pathways. The TD pathway is localized to the germinal centers (Casola et al., 2004) and involves cognate interactions between antigen-specific B cells and CD40 ligand expressing CD4$^+$ T cells with CD40 expressed on B cells (Quezada et al., 2004). Within the GI tract, TD high-affinity IgA-producing plasma cells are optimally generated within the germinal centers of mesenteric LNs and Peyer's patches via TGF-β and IL-21 produced by follicular T helper cells (Dullaers et al., 2009). In the TI pathway of IgA CSR (Macpherson et al., 2000), polyreactive IgA is produced with lower affinity, albeit a shorter latency than IgA produced during TD IgA CSR (Cerutti, 2008).

DCs have been shown to induce both TI and TD IgA responses through the release of several IgA-inducing factors. These include B cell–activating factor (BAFF; also known as BLyS, a proliferation-inducing ligand [APRIL]; Nardelli et

Correspondence to Saurabh Mehandru: saurabh.mehandru@mssm.edu

Abbreviations used: APRIL, a proliferation-inducing ligand; BAFF, B cell–activating factor; CCR9, chemokine receptor 9; CLP, colonic lamina propria; CSR, class-switch recombination; CT, cholera toxin; CTr, cell tracker; FDR, false discovery rate; GALT, gut-associated lymphoid tissue; GF, germ free; GI, gastrointestinal; GLT, germ line transcripts; HI, homing index; LDC, lung DC; MedLN, mediastinal LN; MLN DC, mesenteric LN DC; Mφ, macrophage; RA, retinoic acid; RAR, RA receptor; SIgA, secreted IgA; SILP, small intestinal lamina propria; SkDC, skin draining LN DC; SpDC, splenic DC; SPF, specific pathogen free; TD, T cell dependent; TI, T cell independent.

The Rockefeller University Press $30.00
J. Exp. Med. 2016 Vol. 213 No. 1 53–73
www.jem.org/cgi/doi/10.1084/jem.20150567

The Journal of Experimental Medicine

al., 2001; Litinskiy et al., 2002; Cerutti et al., 2005; He et al., 2007; Xu et al., 2007), and TGFβ1, TNF/iNOS, IL-4, IL-6, and IL-10 in the gastrointestinal (GI) tract (Iwasaki and Kelsall, 1999; Sato et al., 2003; Rimoldi et al., 2005; Mora et al., 2006; Martinoli et al., 2007; Tezuka et al., 2007). In addition, TLR-mediated microbial sensing plays an important role in IgA production in the gut.

Although IgA CSR has been shown to occur in the respiratory mucosa (Sangster et al., 2003; Xu et al., 2008), much remains to be elucidated about lung DC (LDC)–mediated induction and regulation of respiratory IgA production. This is caused, in part, by the heterogeneity of lung APC populations, which have only been functionally defined recently (Langlet et al., 2012; Schlitzer et al., 2013). Although the lungs have been considered sterile, there is an increasing appreciation of microbial communities within murine (Barfod et al., 2013) and human (Huang et al., 2013) lungs. Importantly, the role of microbiome in IgA class-switching in the lung has not been studied to date.

Given that increased understanding of respiratory IgA production may lead to improved mucosal vaccines, we examined the ability of specific lung APC subsets to induce IgA CSR. Moreover, we investigated the impact of the microbiota during lung APC-mediated IgA CSR. In addition to the local generation of IgA, we have examined its dissemination to other organs and ability to mediate protection against infectious challenge. The data presented here provide novel and fundamental insights into the induction of IgA CSR by LDCs and inform the design of novel preventative and therapeutic strategies against mucosal diseases in humans.

RESULTS

Lung CD103$^+$ and CD24$^+$ DCs, but not lung macrophages (Mφs), induce IgA CSR

We first sought to determine that bona fide LDCs were responsible for IgA CSR. MHCII^{hi}CD11c$^+$Siglec-F$^-$ lung cells were collected from enzymatically digested lungs of C57BL/6 mice and FACS sorted. The gating strategy and purity of the populations, consistently >96%, are shown in Fig. S1. Additionally, MHCII^{hi}CD11c^{hi} DCs were FACS isolated from the spleen DCs (SpDCs), mesenteric LN DCs (MLN DCs), and skin-draining LN DCs (SkDCs) and co-cultured with CD43^{neg} CD19$^+$IgM$^+$ B cells at a ratio of 2:1 DC/B cells for 4 d. B cells were stimulated with α-IgM (Wortis et al., 1995) and α-CD40 (Nonoyama et al., 1993; Cerutti, 2008). We observed that the induction of IgA$^+$CD19$^+$ B cells in LDC–B cell co-cultures was similar to MLN DC–B cell co-cultures and significantly greater than SpDC– and SkDC–B cell co-cultures (Fig. S2). In addition, secreted IgA (SIgA) was also quantified in the culture supernatants using IgA ELISA. In line with the flow cytometry data, the level of SIgA in the LDC cultures was similar to the levels of SIgA in MLN DC cultures and significantly higher than the levels in SpDC or SkDC cultures (Fig. S2). Interestingly, MHCII^{lo}CD11c$^+$Siglec-F$^+$ cells putative alveolar Mφs (AM) failed to induce IgA CSR (unpublished data).

IgA CSR is mediated by activation induced cytidine deaminase (AID), a well-documented mammalian DNA-editing enzyme (Muramatsu et al., 2000), which is encoded by the *Aicda* gene. We observed that the level of *Aicda* transcripts were significantly higher in LDC- and MLN DC-cultured B cells compared with SpDC- and SkDC-cultured B cells, or B cells alone (Fig. S2). Additionally, Cα germ line transcripts (GLT; Stavnezer, 1996) were quantified and found to be significantly higher in B cells cultured with LDC and MLN DCs than those cultured with SpDC, SkDC, or B cells alone, further confirming the capacity of LDCs to induce IgA CSR (Fig. S2).

To define which of the lung APC subsets induce IgA CSR, we examined Siglec-F$^-$MHCII^{hi}CD11c$^+$CD103$^+$CD11b$^-$ cells (LDC CD103$^+$), Siglec-F$^-$MHCII^{hi}CD11c$^+$CD103$^-$CD11b$^+$ CD24$^+$ cells (LDC CD24$^+$), and Siglec-F$^-$MHCII^{hi}CD11c$^+$ CD103$^-$CD11b$^+$CD64$^+$ cells (LMφ CD64$^+$) separately based on recently described functional, ontogenetic, and phenotypic criteria to define lung APCs (Langlet et al., 2012; Schlitzer et al., 2013). MLN DCs, SpDCs, and SkDCs were used as controls. LDC CD103$^+$, LDC CD24$^+$, and MLN DC were potent inducers of IgA CSR. In contrast, the LMφ CD64$^+$ were poor at inducing IgA CSR (Fig. 1, A and B). This was further confirmed by IgA quantification within the supernatants (Fig. 1 C). Additionally, LDC CD103$^+$ and LDC CD24$^+$ induced higher levels of *Aicda* (Fig. 1 D) and *Cα GLT* (Fig. 1 E) in B cells compared with LMφ CD64$^+$ and SpDC. We also observed that LDCs induced IgA CSR in the absence of α-CD40 stimulation (which was used here as an in vitro surrogate of TI IgA CSR, albeit with caveats). The levels of IgA produced were expectedly lower in the (–) α-CD40 conditions compared with the (+) α-CD40 conditions (Fig. 1 F). Finally, we also investigated the ability of respective lung APC subsets to induce IgA CSR in the absence of α-CD40 stimulation (Fig. 1 G). Together, these data demonstrate that among the LDC subsets, the LDC CD103$^+$ as well as the LDC CD24$^+$, a subset of the heterogeneous CD11c$^+$MHCII^{hi}CD11b$^+$ population, induce IgA CSR, whereas the LMφ CD64$^+$ (also contained within the CD11c$^+$ MHCII^{hi}CD11b$^+$ cells) do not.

There is strong evidence that lung draining LNs (such as mediastinal LNs [MedLNs]) act as the initial and major sites of B cell response, preceding induction of antibodies in the lungs (Sangster et al., 2003; Sealy et al., 2003). Therefore, we next examined the induction of IgA$^+$ B cells in the lung and draining LNs (MedLNs) at steady state and after immunization and observed a progressive increase in IgA$^+$ B cells in both MedLNs and lungs after i.n. immunization with cholera toxin (CT). Although these data cannot confirm that MedLNs were the site of initial DC–B cell interaction, the fact that MedLN IgA response preceded the response in the lungs is consistent with previous data wherein antibody forming cells are identified in the cervical and MedLN as early as 2–3 d after infection (Sealy et al., 2003; Choi and Baumgarth, 2008; Fig. 1 H).

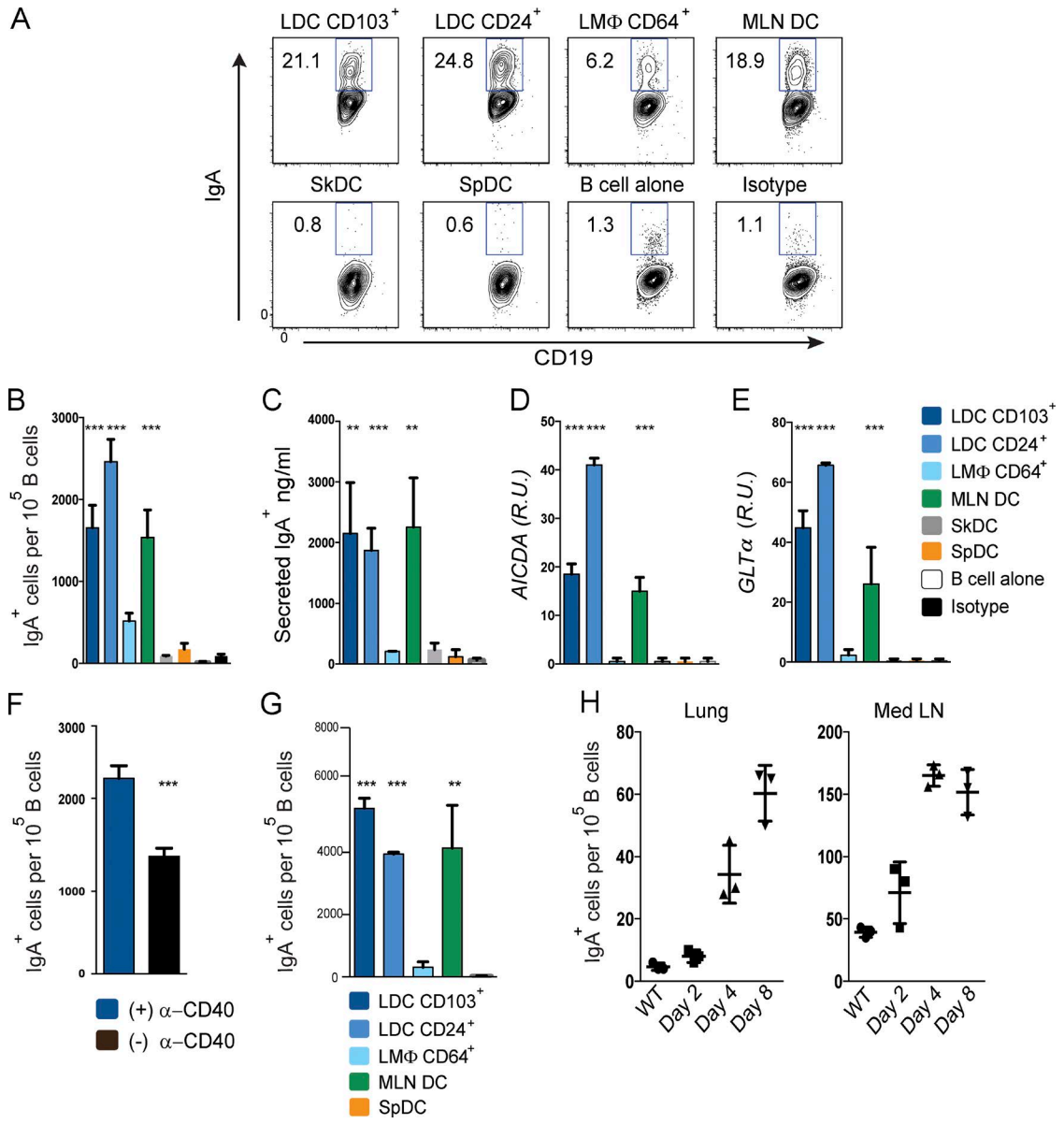

Figure 1. **Lung CD103⁺ and CD24⁺ DCs but not lung Mφs induce IgA CSR.** (A–E) Siglec-F⁻MHCII^{hi}CD11c⁺CD103⁺CD11b⁻ (LDC CD103⁺), Siglec-F⁻MHC II^{hi}CD11c⁺CD103-CD11b⁺CD24⁺ (LDC CD24⁺), and Siglec-F⁻MHCII^{hi}CD11c⁺CD103-CD11b⁺CD64⁺ (LMφ CD64⁺), all isolated from the lungs, SpDC, SkDC, and MLN DCs were cultured with CD43^{neg}CD19⁺IgM⁺ B cells and IgA⁺ B cells were quantified. Data from three experiments is shown with 10 mice pooled per experiment. Statistical comparisons made to LMφ CD64⁺ are shown here. (A) Representative flow cytometry plots. (B) Cumulative data quantifying of the number of CD19⁺IgA⁺ B cells. (C) ELISA quantification of the IgA secreted by B cells in culture. (D and E) qRT-PCR of mRNA isolated from B cells stimulated for 2 d, with the respective DC populations for *AICDA* (d) and *GLT-α* (e). Data are normalized to GAPDH and expressed in relative units. (F) Flow-sorted total LDCs were cultured with CD43^{neg}CD19⁺IgM⁺ B cells either with α-CD40 or without α-CD40 conditions and IgA⁺ B cells were quantified. Cumulative data from three experiments (seven mice per experiment) is shown. (G) Flow-sorted lung APC subsets (LDC CD103⁺, LDC CD24⁺, and LMφ CD64⁺), MLN DCs, and SpDCs were cultured with CD43^{neg}CD19⁺IgM⁺ B cells in (–) α-CD40 conditions and IgA⁺ B cells were quantified. Cumulative data from two experiments (seven mice per experiment) is shown. Statistical comparisons are made to LMφ CD64⁺. (H) Flow cytometric quantification of IgA⁺ B cells in the lung and MedLN at steady state and after immunization with CT. Cumulative data from two experiments (three mice per experiment) is shown. **, $P < 0.01$; ***, $P < 0.001$.

LDC CD103⁺ and LDC CD24⁺ induce IgA CSR in a retinoic acid (RA)– and TGF-β–dependent manner

Having established that LDC CD103⁺ and LDC CD24⁺ induce IgA CSR, whereas LMφ CD64⁺ do not, we examined the mechanisms involved. Global transcriptome analysis was used to compare gene expression levels in the LDC CD103⁺, LDC CD24⁺ and LMφ CD64⁺ subsets. Using the SAM method (Tusher et al., 2001) with a false discovery rate (FDR) thresh-

old of 5%, genes differentially expressed between all pairs of the three lung APCs were compared. Enriched pathways were identified in these gene lists using the DAVID tool (Huang et al., 2009). Among the enriched pathways, the "Intestinal immune network for IgA production" pathway (LDC $CD24^+$ vs. LMφ $CD64^+$; P = 0.04; Benjamini q = 0.2) was investigated further. Most notably, *Tgf-β1*, which was determined to have an unequivocal role in inducing IgA within the GI tract (Stavnezer et al., 2008), was up-regulated in both LDC $CD103^+$ (2.3-fold) and LDC $CD24^+$ (19.2-fold) compared with LMφ $CD64^+$ (Fig. 2 A). Given that TGF-β must be activated to exert its biological effects and that TGF-β mRNA levels do not correspond to active TGF-β protein (Annes et al., 2003), we quantified the expression of TGF-β–activating integrin αvβ8 in sorted LDC/Mφ subsets by qPCR. Both LDC $CD103^+$ and LDC $CD24^+$ expressed significantly higher levels of integrin β8 compared with LMφ $CD64^+$ and SpDCs (Fig. 2 B). These data suggested that LDC $CD103^+$ and LDC $CD24^+$ were equipped with the machinery to convert latent TGF-β into its active form.

Vitamin A deficiency is associated with a selective loss of IgA-producing cells (Mora et al., 2006), and recent reports show that RA acts as a cofactor in IgA CSR (Seo et al., 2013). We specifically examined the role played by RA in IgA CSR by LDCs and examined RAL DH2 (*Aldh1a2*) mRNA transcripts in the unstimulated, flow-sorted LDC and LMφ populations. *Aldh1a2* expression was higher in the LDC $CD103^+$ and LDC $CD24^+$ compared with LMφ $CD64^+$ (Fig. 2 C). These data are concordant with the Immgen Consortium data (Heng and Painter, 2008). Further, addition of a RAR-β inhibitor (RAR-β), LE540 to the DC/B cell cultures resulted in a significant reduction of IgA levels in both LDC $CD103^+$ and LDC $CD24^+$ B cell co-cultures (Fig. 2, D–F) across a range of LE540 concentrations (2.5 µM, 250 nM, and 25 nM).

Finally, having observed differential expression of *Tgf-β1* gene within LDC and LMφ, we investigated the effect of inhibiting TGF β on IgA CSR by LDCs. An α-TGF-β–blocking antibody was added in a range of concentrations on days 0 and 3. This resulted in reduced IgA CSR by the LDC subsets (Fig. 2, G–I). Interestingly, the effect of TGF-β inhibition appeared to be more pronounced in the LDC $CD103^+$ cultures than the LDC $CD24^+$ cultures (Fig. 2, G and H). Furthermore, a dose-dependent TGF-β inhibition was seen with LDC $CD103^+$ but not with LDC $CD24^+$ (Fig. 2 I).

LDC $CD103^+$, LDC $CD24^+$, and LMφ $CD64^+$ all express high levels of APRIL and BAFF

In addition to genes involved in T cell–mediated IgA CSR, we investigated the expression of factors involved in TI IgA CSR, including the TNF family members: APRIL (Hahne et al., 1998) and B lymphocyte stimulator protein (BLys or BAFF; Moore et al., 1999; Litinskiy et al., 2002). Unlike the SpDC, which had negligible levels of APRIL and did not induce IgA CSR, LDC $CD103^+$, LDC $CD24^+$, and LMφ $CD64^+$ all expressed high levels of APRIL protein (Fig. 3 A), with expression being highest in the LDCs $CD24^+$ (Fig. 3 B). APRIL expression was further confirmed using immunohistochemistry. Again, all three lung APC subsets expressed APRIL proteins, in contrast to SpDCs, which lacked APRIL expression (Fig. 3 C). These data were further corroborated by comparing mRNA levels of APRIL and BAFF within sorted lung APC subsets (Fig. 3 D). Incidentally, we observed the highest levels of BAFF mRNA in the LMφ $CD64^+$ compared with LDC $CD103^+$ and LDC $CD24^+$ (Fig. 3 D).

We next studied the effect of inhibiting APRIL and BAFF in vitro. A recombinant mouse TACI-Fc decoy receptor (Schneider et al., 1999; He et al., 2010) was added to the DC/B cell cultures on days 0 and 3. Nonsignificant reduction in IgA CSR was noted in both LDC $CD103^+$ and LDC $CD24^+$ (Fig. 3, E and F). Similar results were observed using $TACI^{-/-}$ B cells (unpublished data). In addition to BAFF and APRIL, we also investigated IL-10 as a potential mediator of LDC-mediated IgA CSR by adding α-IL-10–blocking antibody to the DC/B cell cultures on days 0 and 3. As shown in Fig. 3 (G and H), this did not significantly affect the induction of IgA mediated by LDC $CD103^+$, although a decrease in IgA CSR was observed with the LDC $CD24^+$. Thus, whereas LDC $CD103^+$ and LDC $CD24^+$ induced IgA CSR, and LMφ $CD64^+$ did not, all three lung APC subsets expressed APRIL and BAFF.

To definitively understand the difference between the IgA class-switching ability of LDCs and LMφ, we asked whether IgA CSR by the LMφ $CD64^+$ could be induced by the addition of RA and TGF-β. To this effect, LMφ $CD64^+$ were cultured with IgM^+ B cells with or without TGF-β or TGF-β and RA. TGF-β alone resulted in increased IgA CSR; however, TGF-β and RA had a synergistic affect and induced significantly higher levels of IgA, similar to LDC $CD103^+$ (Fig. 3, I and J). In contrast, addition of APRIL to the LMφ $CD64^+$-B cell cultures failed to induce IgA CSR and no additive effect was observed upon addition of APRIL with TGF-β and RA (Fig. 3 K). Combined, these results show that although LDC $CD103^+$, LDC $CD24^+$, and LMφ $CD64^+$ all express APRIL and BAFF, which are powerful TI IgA class switching molecules, the additional ability of LDC $CD103^+$ and LDC $CD24^+$ to generate TGF-β and RA confers upon them the ability to induce IgA CSR.

Microbiota imprint LDCs with the capacity to induce IgA CSR

Bacterial populations within the gut have been shown to influence IgA CSR via intestinal B cells (Macpherson and Uhr, 2004). To determine the role of microbiota in LDC-mediated IgA CSR, we sorted $MHCII^{hi}CD11c^+Siglec\text{-}F^-$ lung cells from specific pathogen–free (SPF), germ-free (GF), and antibiotic-treated mice and cultured them in the presence of α-IgM– and α-CD40–stimulated $CD43^{neg}CD19^+IgM^+$ B cells (Fig. 4, A and B). Mice were subjected to 4 wk of orally administered combination of antibiotics comprised of

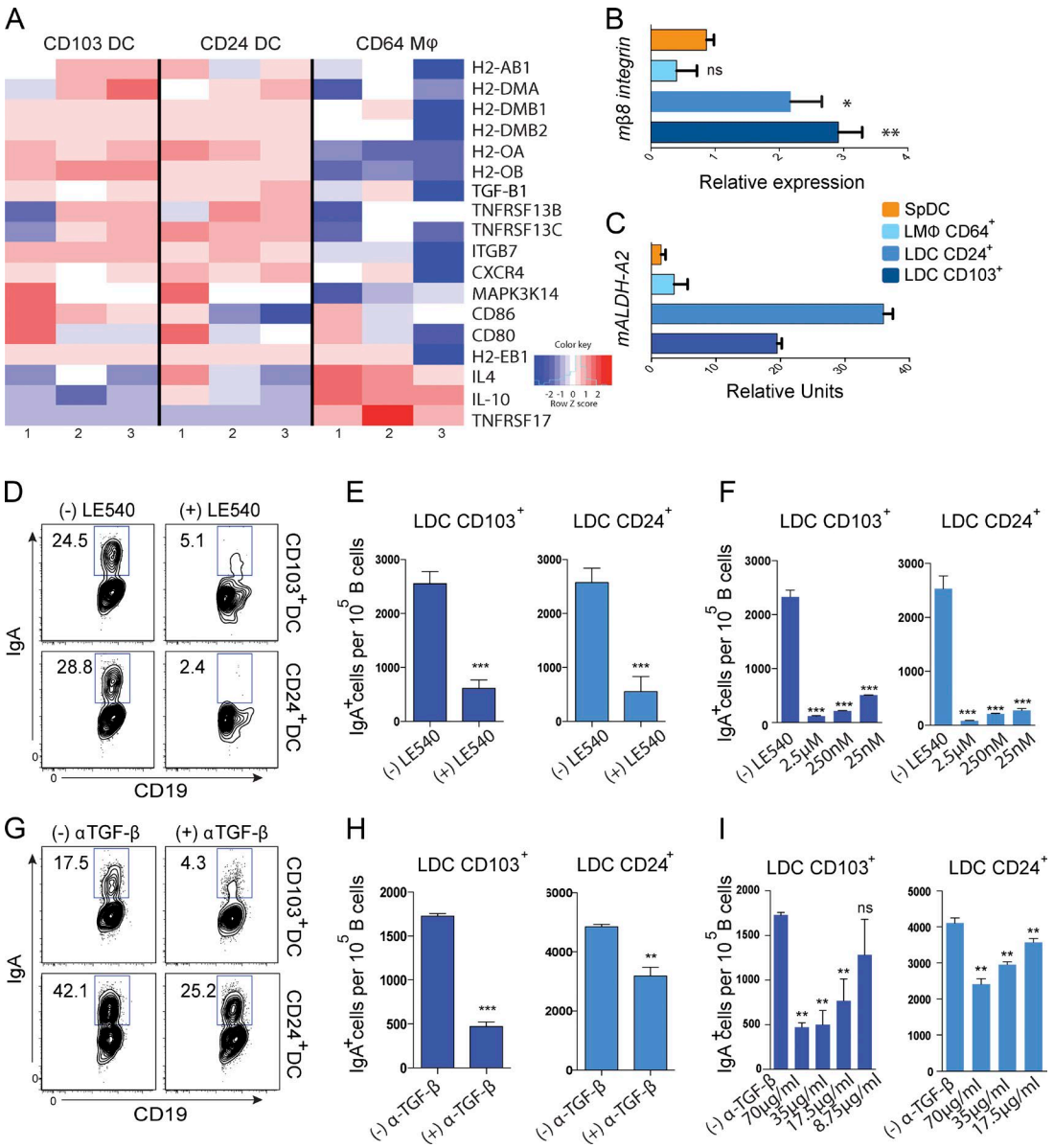

Figure 2. **LDC CD103⁺ and LDC CD24⁺ mediate IgA class switching in an RA– and TGF-β–dependent manner.** (A) Microarray analysis of lung APC subsets. Heat map showing the differential expression of genes in the IgA CSR pathway. Colors correspond to significant fold change expression. Red, high expression; blue, low expression. (B) qRT-PCR of mRNA isolated from flow-sorted LDC CD103⁺, LDC CD24⁺, LMφ CD64⁺, and SpDC, respectively. The expression of Integrin β8 mRNA was normalized to actin and expressed in relative units. (C) qRT-PCR of mRNA isolated from flow-sorted LDC CD103⁺, LDC CD24⁺, LMφ CD64⁺, and SpDC, respectively. The expression of *mAldha2* was normalized to GAPDH and expressed in relative units. (D–F) Flow-sorted LDC CD103⁺ or LDC CD24⁺ were cultured with naive B cells in the absence or presence of the RAR-β inhibitor LE540, and IgA⁺ B cells were quantified. (D) Representative flow cytometry plots. (E) Cumulative data from three different experiments with seven mice pooled per experiment. (F) Escalating doses of LE540 (25 nM, 250 nM, and 2.5 μM) were added to the DC–B cell culture on day 0. Cumulative data from two independent experiments is shown (with seven mice pooled per experiment). Statistical comparisons are made with (–) LE540 condition. (G– I) Flow-sorted LDC CD103⁺ or LDC CD24⁺ were cultured with naive B cells in the absence or presence of α-TGF-β neutralizing antibody, and IgA⁺ B cells were quantified. (G) Representative flow cytometry plots. (H) Cumulative data from three different experiments with seven mice pooled per experiment. (I) Escalating doses of α-TGF-β neutralizing antibody (8.75, 17.5, 35, and 70 μg/ml) were added to the DC–B cell cultures on days 0 and 3. Cumulative data from two independent experiments (with seven mice pooled per experiment) is shown. Statistical comparisons are made with (–) α-TGF-β condition. *, $P < 0.05$; **, $P < 0.01$; ***, $P < 0.001$.

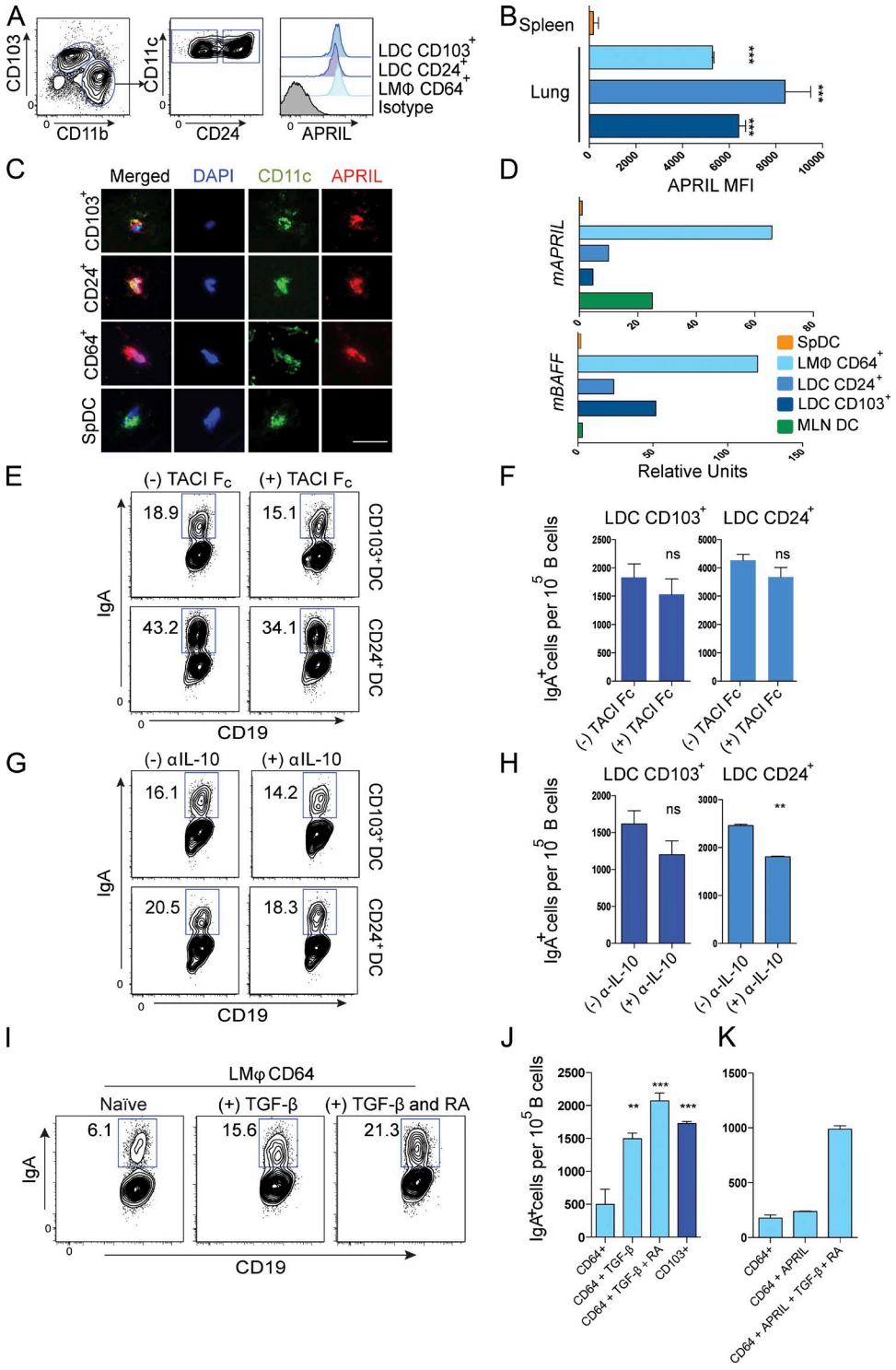

Figure 3. **LDC CD103$^+$, LDC CD24$^+$, and LMΦ CD64$^+$ cells all express high levels of APRIL and BAFF.** (A) Representative flow cytometry plots comparing the expression of APRIL protein in lung APC subsets. (B) Cumulative data comparing the mean fluorescence intensity (MFI) of APRIL expression. Three independent experiments are shown here with three mice per experiment. Statistical comparisons are made to SpDCs. (C) Immunofluorescent analysis of APRIL expression on sorted, LDC CD103$^+$, LDC CD24$^+$, LMφ CD64$^+$, and SpDCs where DAPI is shown in blue, CD11c in green, and APRIL in red. Bar, 10 µm. (D) qRT-PCR of mRNA isolated from flow-sorted LDC CD103$^+$, LDC CD24$^+$, LMφ CD64$^+$, MLN DCs, and SpDCs comparing the expression of *mAPRIL* (top) and *mBAFF* (bottom). Data are normalized to GAPDH and expressed in relative units. (E and F) Flow-sorted LDC CD103$^+$ or LDC CD24$^+$ were cultured with CD43^{neg}CD19$^+$IgM$^+$ B cells in the absence or presence of TACI-Fc antibody added on culture days 0 and 3. (E) Representative flow cytometry plots.

vancomycin, neomycin, metronidazole, and ampicillin. This treatment resulted in significant changes in the composition of culturable commensal bacteria in the gut (unpublished data). Interestingly, IgA CSR was significantly reduced in the GF LDCs and antibiotic-treated LDCs compared with SPF LDCs. This was further confirmed with SIgA quantification within the supernatants (Fig. 4 C). Additionally, the levels of *Aicda* and *Cα GLT* were significantly reduced in B cells cultured with GF LDCs compared with SPF LDCs. There was a reduction in antibiotic-treated mice, but the differences did not reach statistical significance (Fig. 4, D and E). These data suggest that commensal microbiota influenced the capacity of LDCs to mediate IgA CSR.

To better understand the mechanisms involved, global transcriptome analysis was used to compare gene expression levels between SPF and GF LDC subsets. Examination of the "Immune network for IgA production" pathway revealed several differentially expressed genes, with the most notably down-regulated genes within GF lung APCs being *Tgf-β1* and *Aldh1a2*. Strikingly, $CD24^+$ LDC from GF mice expressed 24-fold lower levels of TGF-β1 compared with $CD24^+$ LDC from SPF mice (Fig. 4 F), whereas the expression of *Aldh1a2* was decreased by 2.3-fold.

Having observed a significant reduction in the ability of LDC from GF and antibiotic-treated mice to induce IgA CSR, we sought to determine ways to rescue the class switching function of LDCs from antibiotic-treated mice. SPF mice were maintained on the antibiotic cocktail long term (12 wk). At week 12, half of the mice were gavaged with 100 µg of LPS daily for 5 d, whereas the other half were gavaged with 100 µg of PBS daily for 5 d. 12-wk antibiotic treatment further reduced the ability of LDCs to induce IgA CSR (Fig. 4 G) to levels observed in GF mice. Oral administration of LPS completely restored LDC IgA CSR to SPF levels. To corroborate the LPS data, we asked whether reconstitution of GF mice with WT (SFP) microbial flora could restore LDC's capacity to mediate IgA CSR. Remarkably, reconstitution of GF mice with cecal contents from SPF mice for 2 wk was sufficient to restore the IgA CSR ability (Fig. 4, H and I). Based on this set of experiments, we conclude that microbial signals profoundly affect the ability of LDC to induce IgA class switching.

LDC-mediated IgA CSR is MyD88 and TRIF dependent

We next examined the mechanisms by which microbial signals imprint IgA class-switching function on LDCs. Because pattern recognition receptors are essential in cellular response to microbial stimuli, we studied the IgA switching function of LDCs from $TRIF^{-/-}MyD88^{-/-}$ mice. Strikingly, in the absence of TLR signaling, the IgA class switching function of LDCs was completely abolished (Fig. 5, A–C). *Aicda* and *Cα GLT* levels were also significantly reduced in B cells stimulated with $TRIF^{-/-}MyD88^{-/-}$ LDC (Fig. 5, D and E). The adaptor protein MyD88 is recruited by TLR1, TLR 2, TLR 4, TLR5, TLR6, TLR7, and TLR 9, whereas TRIF is recruited by TLR3, TLR4, and TLR5 (O'Neill et al., 2013). To further understand the specific pathways involved, we examined $TRIF^{-/-}$ and $MyD88^{-/-}$ single knockout mice. Although inhibition of TRIF signaling partially impaired LDC IgA CSR (Fig. 5, F and G), inhibition of MyD88 signaling alone completely abrogated the IgA class switching function of LDCs. Collectively, these data indicate that TLR signaling, mediated through the MyD88 adaptor protein, is essential for LDCs to induce IgA CSR.

Having observed that the TGF-β1 gene was highly down-regulated in the LDC from GF mice compared with SPF mice, we sought to examine if lack of TLR signaling reduces TGF-β production. The levels of active TGF-β1 protein produced by GF and $TRIF^{-/-}MyD88^{-/-}$ LDCs were quantified after a 5-d culture. We found a significant reduction in active TGF-β1 production by both GF and $TRIF^{-/-}MyD88^{-/-}$ LDCs compared with SPF LDC in vitro (Fig. 5 H). Reduced levels of active TGF-β1 were also detected in the lung tissues of these animals (unpublished data).

Next, we asked whether the IgA CSR by $TRIF^{-/-}MyD88^{-/-}$ LDCs could be restored by the addition of TGF-β1. As demonstrated in Fig. 5 (I and J) supplementation of the $TRIF^{-/-}MyD88^{-/-}$ LDC cultures with TGF-β1 restored the level of IgA^+ B cells to that seen with WT DCs. In contrast, while addition of TGF-β to SpDC increased the IgA^+ B cells compared with SpDC alone, the levels remained significantly lower than LDC from WT mice. Finally, we asked whether the lack of IgA CSR in $TRIF^{-/-}MyD88^{-/-}$ LDC was a result of impaired production of RA. We added RA to $TRIF^{-/-}MyD88^{-/-}$ LDC in vitro and observed that the level of $CD19^+IgA^+$ cells increased significantly compared with $TRIF^{-/-}MyD88^{-/-}$ DCs alone. Supplementation of TGF-β1 resulted in significantly enhanced production of IgA, approaching the levels seen with WT LDCs (Fig. 5, I and J). Together, these data demonstrate a critical, TGF-β1–dependent role of MyD88-dependent TLR signaling in the IgA class switching function of LDC.

(F) Cumulative data from two independent experiments with seven mice pooled per experiment. (G and H) Flow cytometric analyses showing the effect of blocking IL-10 on LDC-induced IgA CSR. Flow-sorted LDC $CD103^+$ or LDC $CD24^+$ were cultured with naive B cells in the absence or presence of α-IL-10 neutralizing antibody added on culture days 0 and 3, and IgA^+ B cells were quantified. (G) Representative flow cytometry plots. (H) Cumulative data from two independent experiments with seven mice pooled per experiment. (I–K) Flow-sorted LMφ $CD64^+$ were cultured with $CD43^{neg}CD19^+IgM^+$ B cells in the indicated conditions, and IgA^+ B cells were quantified. (I) Representative flow cytometry plots. (J) Cumulative data from three different experiments with seven mice pooled per experiment. Statistical comparisons are made to LMφ $CD64^+$ alone. (K) Cumulative data from two individual experiments with six mice pooled per experiment. Statistical comparisons are made to LMφ $CD64^+$ alone. **, $P < 0.01$; ***, $P < 0.001$.

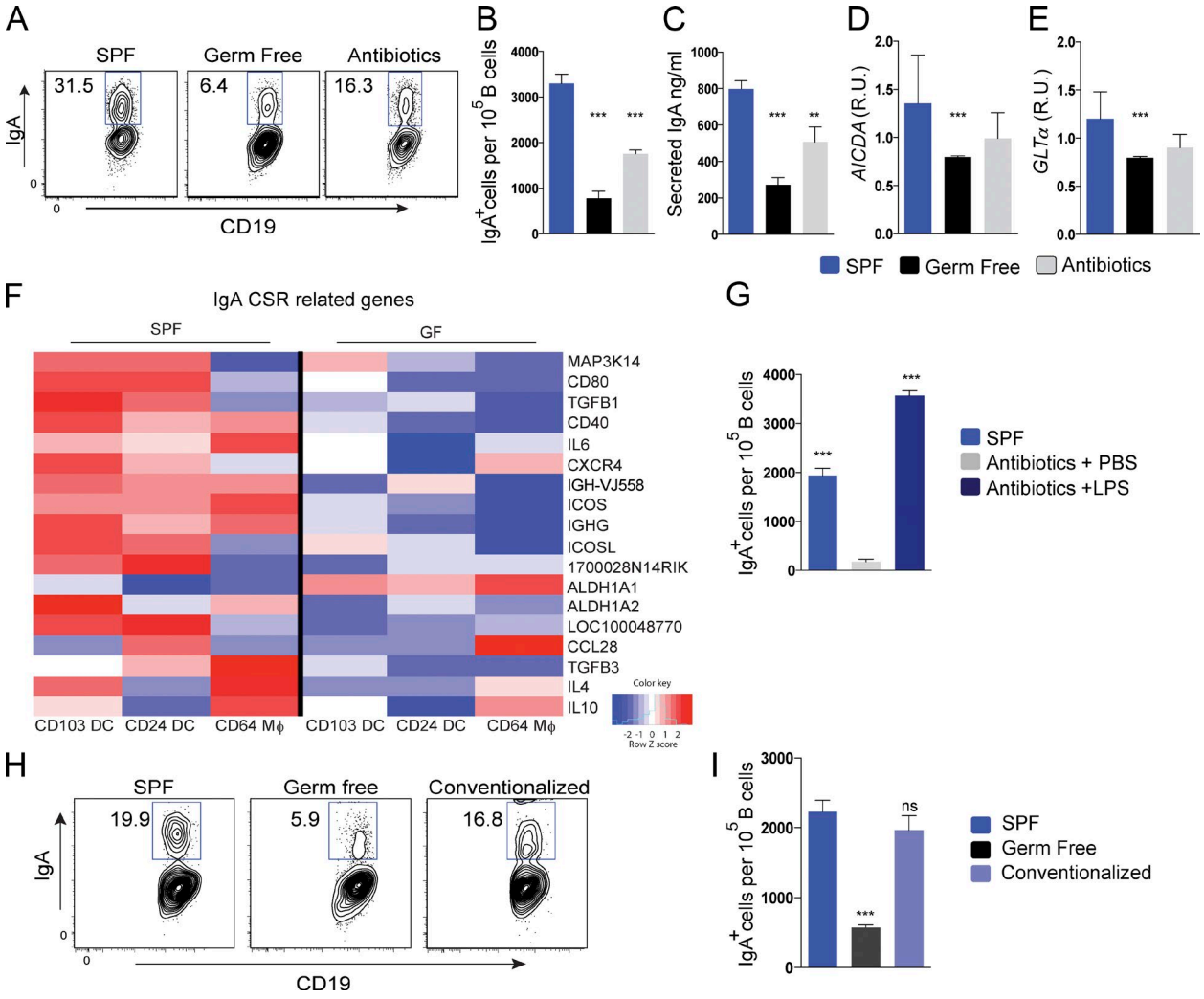

Figure 4. **Microbiota imprint LDCs with the capacity to mediate IgA CSR.** (A–E) Flow sorted LDCs (defined as MHCII^{hi}CD11c^{+}Siglec-F^{-}CD64^{-} cells) were cultured with CD43^{neg}CD19^{+}IgM^{+} B cells and IgA^{+} B cells were quantified. Data from three experiments with seven mice pooled per experiment are shown. Statistical comparisons are made to SPF mice. (A) Representative flow cytometry plots. (B) Cumulative data. (C) ELISA to quantify the levels of IgA secreted by B cells in culture. (D and E) qRT-PCR of mRNA isolated from B cells stimulated for 2 d with the respective DC populations for *AICDA* (D) and *GLT-α* (E). Data are normalized to GAPDH and expressed in relative units. (F) Microarray analysis comparing LDCs from SPF and GF mice. Heat map showing the differential expression of genes in the IgA CSR pathway. Colors correspond to significant fold change expression. Red, high expression; blue, low expression. (G) LDCs from SPF mice, mice treated with oral antibiotics for 12 wk + oral PBS for 5 d, and mice treated with oral antibiotics for 12 wk + oral LPS for 5 d were cultured with CD43^{neg}CD19^{+}IgM^{+} B cells and IgA^{+} B cells were quantified. Cumulative data from two independent experiments with seven mice pooled per experiment are shown. Statistical comparisons are made to the antibiotics + PBS group. (H and I) LDCs from SPF mice, GF mice, and GF mice conventionalized with the cecal contents of SPF mice were cultured with CD43^{neg}CD19^{+}IgM^{+} B cells and IgA^{+} B cells were quantified. (H) Representative flow cytometry plots. (I) Cumulative data from two independent experiments, with five mice pooled per experiment. Statistical comparisons are made to the SPF group. **, $P < 0.01$; ***, $P < 0.001$.

LDCs induce expression of gut-homing molecules on IgA^{+} cells and license B cell migration to the GI tract

After CSR, B cells need to migrate to the mucosal sites to perform effector functions. Mora et al. (2006) have demonstrated that gut-associated lymphoid tissue (GALT)–resident-DCs metabolize vitamin A to RA and induce gut-homing receptors on B cells. Because we (Ruane et al., 2013) and others (Guilliams et al., 2010) have shown that LDCs can also metabolize vitamin A, we investigated the ability of LDCs to induce gut-homing signals on B cells. We examined total LDCs (identified as MHCII^{hi}CD11c^{+}Siglec-F^{-} cells) and compared with SpDCs, MLN DCs, and SkDCs for their ability to induce gut-homing signals on CD45^{+}CD43^{neg}CD19^{+} B cells (DC/B cell ratio of 2:1; cultured for 5–7 d). The expression of α4β7 and CCR9 was significantly up-regulated by LDCs, similar to MLN DCs (Fig. 6, A–C). The addition

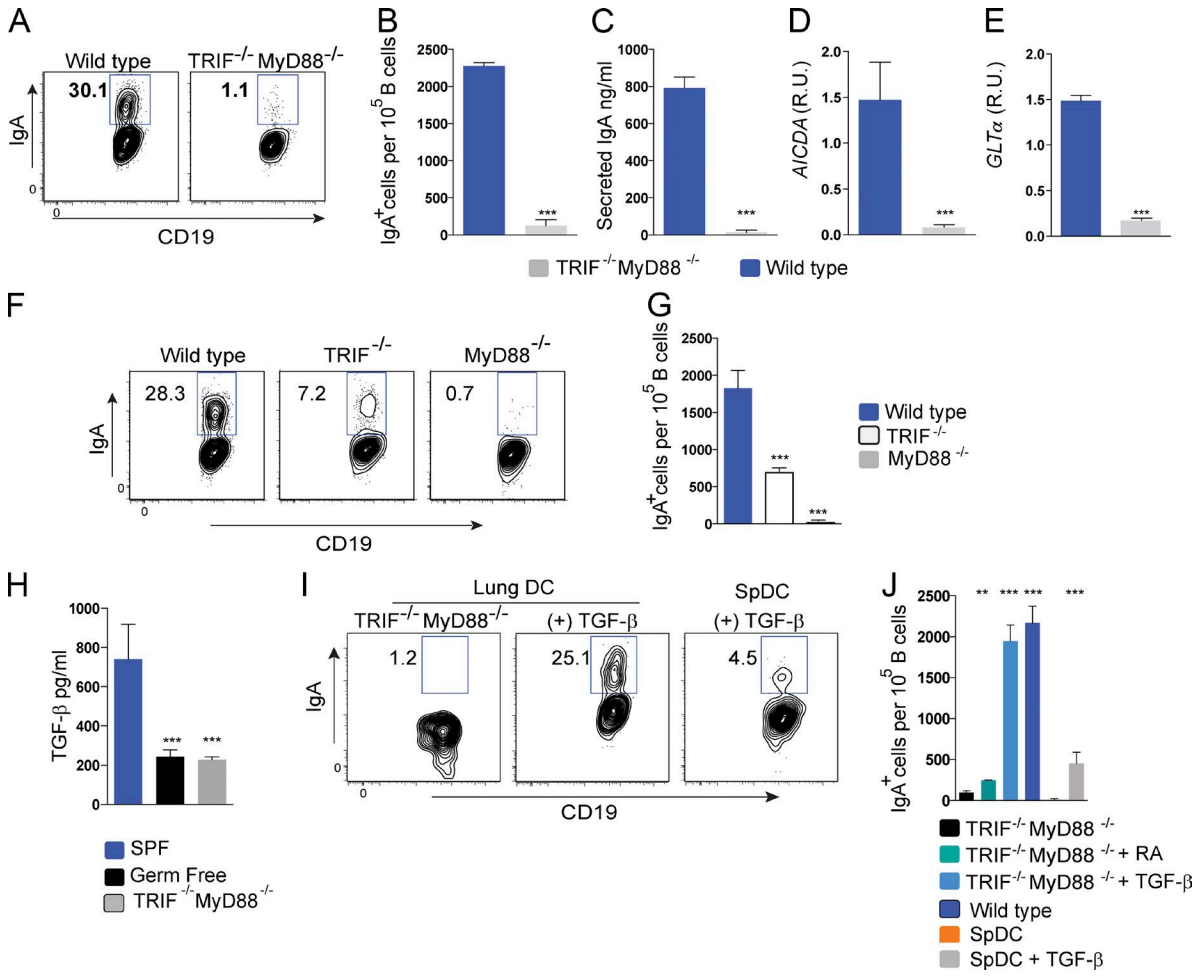

Figure 5. **LDC-mediated IgA CSR is MyD88 and TRIF dependent.** (A–E) LDCs from WT or TRIF$^{-/-}$MyD88$^{-/-}$ mice were cultured with CD43^{neg}CD19^{+}IgM^{+} B cells and IgA^{+} B cells were quantified. Data from three individual experiments with 10 mice pooled per experiment is shown. Statistical comparisons to WT mice are shown. (A) Representative flow cytometry plots. (B) Cumulative data. (C) ELISA to quantify the levels of IgA secreted by B cells in culture. (D and E) qRT-PCR of mRNA isolated from B cells stimulated for 2 d with the respective DC populations for *AICDA* (D) and *GLT-α* (E). Data are normalized to GAPDH and expressed in relative units. (F and G) LDCs from WT, TRIF$^{-/-}$, and MyD88$^{-/-}$-deficient mice were cultured with CD43^{neg}CD19^{+}IgM^{+} B cells and IgA^{+} B cells were quantified. Data from two independent experiments with five mice pooled per experiment are shown. Statistical comparisons were made to WT mice. (F) Representative flow cytometry plots. (G) Cumulative data. (H) ELISA to quantify TGF-β1 produced by LDCs from SPF, GF, and TRIF$^{-/-}$MyD88$^{-/-}$ mice after 5 d of culture. Statistical comparisons to SPF mice are shown. (I and J) Flow-sorted TRIF$^{-/-}$MyD88$^{-/-}$ LDC and SpDC were cultured with CD43^{neg}CD19^{+}IgM^{+} B cells in the indicated conditions and IgA^{+} B cells were quantified. Statistical comparisons to TRIF$^{-/-}$MyD88$^{-/-}$ mice are shown. (I) Representative flow cytometry plots. (J) Cumulative data from three different experiments with five mice pooled per experiment. **, $P < 0.01$; ***, $P < 0.001$.

of an RAR-β antagonist, LE540, decreased the expression of both α4β7 and CCR9 by LDC and MLN DC stimulated B cells (Fig. 6, D–E). Therefore, we conclude that LDCs induce gut-homing molecules on B cells, mediated by RA signaling.

Next, we investigated whether the induction of the gut-homing molecule, α4β7 is specific to IgA class-switched cells. Upon culture of CD43^{neg}CD19^{+}IgM^{+} B cells with LDC, SpDC, SkDC, and MLN DC (DC/B cell ratio, 2:1), the expression of α4β7 on IgA^{+} B cells was compared with IgA^{-} B cells. Notably, α4β7 expression was comparable between IgA^{+} and IgA^{-} B cells (Fig. 6 F). Additionally, LDC-induced IgA-positive cells (and total B cells; unpublished data) had higher expression of α4β7 than SpDC and SkDC, but lower than MLN DC–cultured B cells (Fig. 6, F and G). To determine if α4β7 and CCR9 induction occurred in a cell contact–dependent manner, LDC-, SpDC-, SkDC-, and MLN DC–conditioned media were added to α-IgM– and α-CD40–stimulated B cells and the induction of α4β7 and CCR9 was investigated. LDC-conditioned medium significantly up-regulated gut-homing molecules, equivalent to MLN DC–conditioned medium (unpublished data). Therefore, LDC-mediated gut-homing molecules are induced in a contact-independent manner, which could explain why the induction of α4β7 was equivalent between IgA^{+} and IgA^{-} B cells.

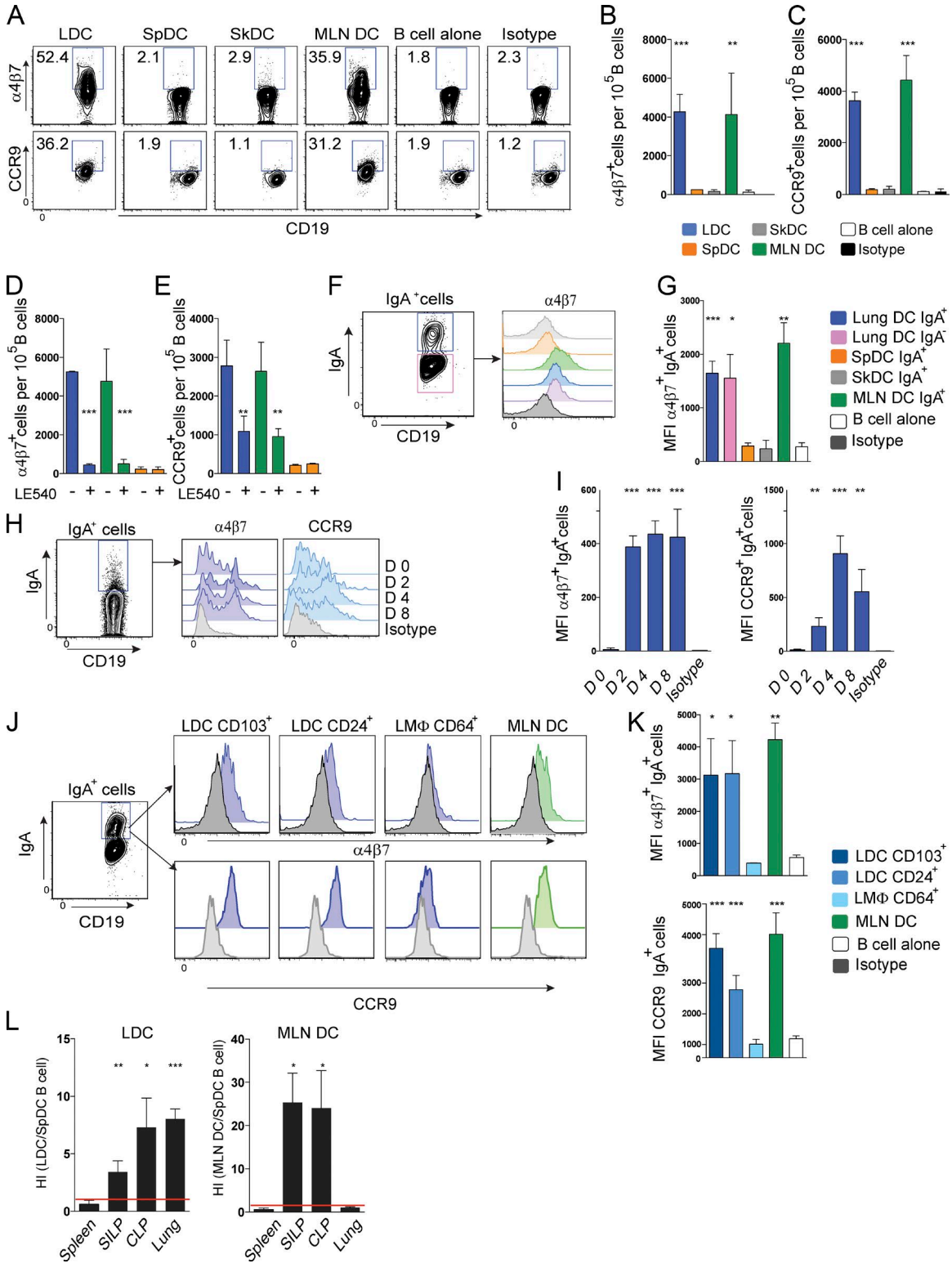

Figure 6. **LDCs induce integrin α4β7 and CCR9 on B cells in a RA dependent manner.** (A–C) Flow-sorted LDCs, SpDCs, SkDCs, and MLN DCs were cultured with α-IgM– and α-CD40–stimulated CD43^{neg}CD19^{+} B cells in a DC/B cell ratio of 2:1 for 5–7 d, and the expression of integrin α4β7 and chemokine receptor CCR9 was measured. Data from three experiments, six mice pooled per experiment, are shown. Statistical comparisons to SpDC are shown. (A) Representative flow cytometry plots. (B) Quantification of α4β7^{+} B cells showing cumulative data. (C) Quantification of CCR9^{+} B cells showing cumulative data. (D and E) Flow-sorted LDCs, MLN DCs, and SpDCs were cultured with CD43^{neg}CD19^{+} B cells in the absence or presence of RAR-β inhibitor LE540,

In addition to the in vitro studies, we also examined the induction of gut-homing molecules on IgA^+ B cells in the lung ex vivo at steady state and after i.n. vaccination. As shown in Fig. 6 (H and I), the expression of α4β7 and CCR9 by IgA^+ B cells significantly increased on days 2, 4, and 8 after i.n. vaccination compared with baseline.

We then asked if there was a difference between the LDC subsets in their ability to induce expression of integrin α4β7 and chemokine receptor 9 (CCR9) on B cells. LDC $CD103^+$ and LDC $CD24^+$ subsets, as well as LMφ $CD64^+$, were cultured with B cells and the expression of α4β7 and CCR9 was quantified. LDC $CD103^+$ and LDC $CD24^+$ both up-regulated integrin α4β7 and CCR9 on B cells, whereas LMφ $CD64^+$ did not (Fig. 6, J and K).

Given the capacity of LDCs to induce gut-homing molecules in vitro and ex vivo, we hypothesized that this mechanism might target B cells to the GI tract in vivo. LDCs and SpDCs, and MLN DCs and SpDCs, were cultured with $CD45.2^+CD43^{neg}CD19^+IgM^+$ B cells for 5 d, and the respective B cells were labeled with CFSE or cell tracker (CTr) and i.v. co-transferred into $CD45.1^+$ recipient mice. Homing index (HI) was calculated as output CFSE:CTr/input CFSE:Ctr for each of the organs examined. As shown in Fig. 6 L, the HI in spleen was 0.9. In contrast, the HI in the small intestinal lamina propria (SILP), colonic lamina propria (CLP), and lung was 3.7, 7.6, and 8.2, respectively. These data demonstrate that, in contrast to SpDC-cultured B cells, LDC-cultured B cells home preferentially to the SILP, CLP, and lung. As previously published (Mora et al., 2006), we found that MLN-stimulated B cells homed more efficiently to the CLP and SILP but not to the spleen or the lung (Fig. 6 L). Thus, LDCs have the capacity to induce gut-homing molecules on IgA^+ B cells, mediating efficient trafficking of B cells to GI effector compartments.

LDCs induce protective IgA in the GI tract

Having observed that LDCs can induce IgA CSR, confer a gut-homing phenotype, and direct the migration of B cells to the GI tract, we wanted to address whether targeting LDCs can mediate protective immunity in the GI tract. For this we used a CT-induced diarrhea model (Tokuhara et al., 2010) characterized by cAMP-induced secretion of water and chloride ions into the small intestine (Spangler, 1992). CT-specific secretory IgA (sIgA) in the intestinal lumen is responsible for protective immunity against CT-induced diarrhea (Tokuhara et al., 2010). Mice were either left untreated (WT+CT) or immunized with CT delivered intranasally (i.n.), intratracheally (i.t.), s.c., or per orally (p.o.). Notably, the i.t. route was specifically chosen to compare with i.n. immunization to minimize possible GI exposure of the i.n.-delivered vaccine. To determine the optimal volume of vaccine antigen, we conducted targeting experiments where C57BL/6 mice were vaccinated i.n. with 50 µg OVA-AF647 delivered either in a volume of 5 or 40 µl. In a volume of 5 µl OVA-AF647, there was no detectable signal in the LDC subsets. In contrast, 40 µl of OVA-AF647 targeted LDCs effectively (Fig. S3 A). To exclude inadvertent GI exposure of the i.n. delivered vaccine, further targeting experiments were performed where we examined antigen-presenting cells in the spleen, MLN, or GI tissue at various time points after i.n. delivery of 40 µl of a fluorescently labeled antibody. Notably, we did not detect antibody-labeled cells in the spleen, MLN, or GI tissues up to 72 h after administration of the i.n. vaccine; however, labeling in the lung and MedLN remained robust (Fig. S3 B). Guided by these targeting experiments, the i.n. vaccine was delivered in a volume of 40 µl. On day 14, mice were challenged orally by administering CT by gavage. At 2.5 h after CT challenge, mice were sacrificed and the weight of the small intestine and its fluid content was determined. We observed that CT immunization delivered via the s.c. route did not result in protection against CT challenge. In contrast, i.n or i.t. delivery of the CT vaccine generated protective immunity against CT challenge, which was comparable in degree to WT and p.o. vaccinated animals (Fig. 7 A). Additionally, we measured anti-CT antibodies in the serum, spleen, and stool of the vaccinated mice. Although s.c. immunization induced strong IgG responses in the serum, it failed to elicit detectable anti-CT IgA in the stool. In contrast, i.n. and i.t. vaccinated

and α4β7 and CCR9 were quantified. Cumulative data from three experiments with six mice pooled per experiment are shown. Statistical comparisons to the respective (–) LE540 condition are shown. α4β7-expressing B cells (D) and CCR9-expressing B cells (E) induced by the respective DC populations. (F and G) Flow-sorted LDCs, SpDCs, SkDCs, or MLN DCs were cultured with $CD43^{neg}CD19^+$ B cells and the expression of integrin α4β7 was measured. (F) Representative flow cytometry plots. (G) Cumulative data from three experiments with six mice pooled per experiment. Statistical comparisons to SpDC are shown. (H and I) Mice were immunized with CT and the expression of $\alpha4\beta7^+$ and $CCR9^+IgA^+$ cells was examined at serial time points. (H) Representative flow plots. (I) Cumulative data from three experiments (three mice per experiment) quantifying the MFI of $\alpha4\beta7^+$ and $CCR9^+$ on IgA^+ B cells. Statistical comparisons to day 0 are shown. (J and K) Flow sorted LDC $CD103^+$, LDC $CD24^+$, LMφ $CD64^+$, or MLN DCs were cultured with $CD43^{neg}CD19^+$ B cells, and the expression of integrin α4β7 on IgA^+ B cells was examined. (J) Representative flow cytometry plots comparing the respective lung APC subsets with IgG 2aκ isotype control. (K) Cumulative data from three independent experiments shown (with five mice pooled per experiment). Statistical comparisons to B cell alone condition are shown. (L) Flow-sorted LDCs and SpDCs (left) or MLN DCs and SpDCs were cultured $CD43^{neg}CD19^+$ $CD45.2^+$ B cells. After culture, 5×10^5 LDC B cells per culture condition were labeled with green (CFSE) and red (CTr) dyes, respectively, mixed in a 1:1 ratio, and adoptively transferred into $CD45.1^+$ mice. After 18 h, CD45.2-gated transferred cells were measured in the spleen, SILP, CLP, and lungs, and the output ratio of LDC-stimulated, CFSE-labeled B cells versus SpDC-stimulated, CTr-labeled B cells was determined. The HI was represented as the yield of CFSE-labeled cells/CTr-labeled cells divided by the input ratio of CFSE-labeled cells/CTr-labeled cells. Cumulative data from three individual experiments is shown (with five mice per experiment). Red line indicates a HI ∼1. Statistical comparisons to spleen HI are shown. *, $P < 0.05$; **, $P < 0.01$; ***, $P < 0.001$.

mice developed CT-specific IgA in stool and serum, as well as a serum IgG response (Fig. 7 B).

To exclude the possibility that serum IgA could have been transported in the bile to the GI tract, we examined the frequency of antigen-specific B cells within the lung and GI tissues using CT-specific ELISPOT. Both i.n. and i.t. immunization resulted in the generation of CT-specific B cells in the GI tissue (Fig. 7 C). To further examine if the nasally delivered vaccine was leading to GI tract exposure, we compared i.n. immunized mice with i.t and sublingual (s.l.) immunized mice. Notably s.l. vaccination induced CT-SIgA in the stool and serum, albeit at a significantly lower level than i.n. and i.t. vaccination (Fig. 7 D). The finding that i.n. and i.t. vaccination both induce protective immunity against CT induced-diarrhea prompted us to investigate whether targeting LDCs modifies the outcome of the humoral immune response. To this effect, CT was administered i.n. at a volume of either 5 or 40 µl (with the dose of antigen being constant). We determined that immunization using a volume of 5 µl and targeting only nose-associated lymphoid tissue DCs was insufficient to induce protective immunity in the GI tract (Fig. 7, E and F). Additionally, CT-specific IgA was significantly lower in both stool and serum samples from these animals (Fig. 7 F). Therefore, targeting of the LDC populations is required to induce protective IgA immunity in the GI tract.

To assess the in vivo contribution of LDCs to IgA induction, we immunized *Batf3*$^{-/-}$ mice lacking CD103$^+$ DCs (Hildner et al., 2008) and WT mice with CT and serially examined the induction of IgA$^+$ B cells in the lung and MedLN. A significant reduction in IgA$^+$ cells was seen in the lung and MedLN of *Batf3*$^{-/-}$ mice compared with WT mice after i.n. immunization (Fig. 7 G). Next, CT-immunized (delivered i.n. or i.t.) WT or *Batf3*$^{-/-}$ mice were challenged orally with CT. *Batf3*$^{-/-}$ mice showed reduced protection after i.n. and i.t. immunization, which was associated with significantly lower levels of stool and serum IgA compared with WT mice (Fig. 7, H and I). These data demonstrate a critical role for *Batf3*$^+$ DCs in the induction of IgA responses, which cannot be compensated for by CD24$^+$ DCs.

To determine if i.n. vaccination could lead to a protective immune response in the gut in the absence of T cell help, TCR$^{-/-}$ mice were immunized i.n. with CT and challenged orally after 14 d. As shown in Fig. 7 J, whereas unimmunized, CT-challenged mice had significantly greater intestinal weight because of the accumulation of enteric fluid, immunized TCR$^{-/-}$ mice were protected against CT challenge.

Finally, having determined a profound effect of microbiota on the production of IgA antibodies by LDC, we assessed the physiological contribution of the microbiota during i.n. vaccination. Using the CT-induced diarrhea model, WT (SPF conditions) and GF mice were immunized with CT delivered i.n. and challenged on day 14. Due to the fact that intestinal weight of GF mice is significantly greater than WT mice (because GF mice accumulate fluid in the intestinal lumen; Fig. 7 K), we focused on CT-specific IgA in the stool and observed significantly reduced levels of CT-specific IgA in the stool, lung, and serum of GF mice compared with SPF mice (Fig. 7 L). These data demonstrate that the efficacy of i.n. vaccination is significantly modulated by the microbiota.

DISCUSSION

Induction of a robust antibody response through mucosal vaccination offers many advantages, including inhibition of microbial adherence, neutralization of toxins, opsonization of bacteria, targeting of antigen to APCs, and antibody-dependent cellular cytotoxicity (Nimmerjahn and Ravetch, 2006; Cerutti and Rescigno, 2008). IgA is the predominant antibody at mucosal surfaces. Therefore, an understanding of the signals that regulate IgA CSR is critical to the design of effective mucosal vaccines. With this as our guiding principle, we undertook this study to determine the factors that influence the production of IgA after i.n. vaccination and have made the following observations.

First, bona fide LDCs, both LDC CD103$^+$ and LDC CD24$^+$, are proficient in inducing IgA CSR, whereas the closely related LMφ CD64$^+$ are not. Second, microbial stimuli, acting through MyD88-dependent TLRs, induce the IgA class-switching function of LDCs via the production of TGF-β. Third, LDCs can up-regulate integrin α4β7 and CCR9 in a RA-dependent fashion, direct antigen-specific B cells to the GI tract, and mediate protection against enteric pathogens after i.n. vaccination. Finally, microbial factors impact the protective effect of i.n. vaccination, demonstrating a bidirectional cross talk between lung and gut immunity.

In contrast to the well-studied process of IgA CSR by gut DCs (Macpherson and Uhr, 2004; He et al., 2007; Tsuji et al., 2008), there are limited studies examining the induction of IgA by LDCs (Wilkes and Weissler, 1994; Naito et al., 2008; Suzuki et al., 2012), with inconsistent results (Wilkes and Weissler, 1994; Naito et al., 2008). This is partly because the description of LDC has been hampered by the overlapping expression of phenotypic markers on bona fide DCs and Mφ in the lung (Ginhoux et al., 2009). Recent studies have clarified this issue such that the expression of CD24 and CD64 on Siglec-F$^-$CD11c$^+$MHCII^{hi}CD11b$^+$ cells distinguishes LDCs from LMφ contained within the heterogeneous, previously called CD11b$^+$ LDC (Schlitzer et al., 2013). Using the same stringent criteria to define LDCs (purity of respective populations in our assays was >96%), we used both molecular indicators of IgA CSR (*aicda* induction and Cα GLT production) and protein quantification of cellular and soluble IgA to document the IgA CSR function of LDC. Through these complementary but distinct assays, we were able to conclude that whereas LDC CD103$^+$ and LDC CD24$^+$ induce robust IgA CSR, LMφ CD64$^+$ are significantly less proficient. To our knowledge, this is the first study distinguishing bona fide LDC and LMφ in their ability to induce IgA class switching.

Further, we found that LDCs induced IgA CSR in both TD and TI conditions, although TI conditions produced less IgA than TD conditions. Notably, much of the data on respiratory

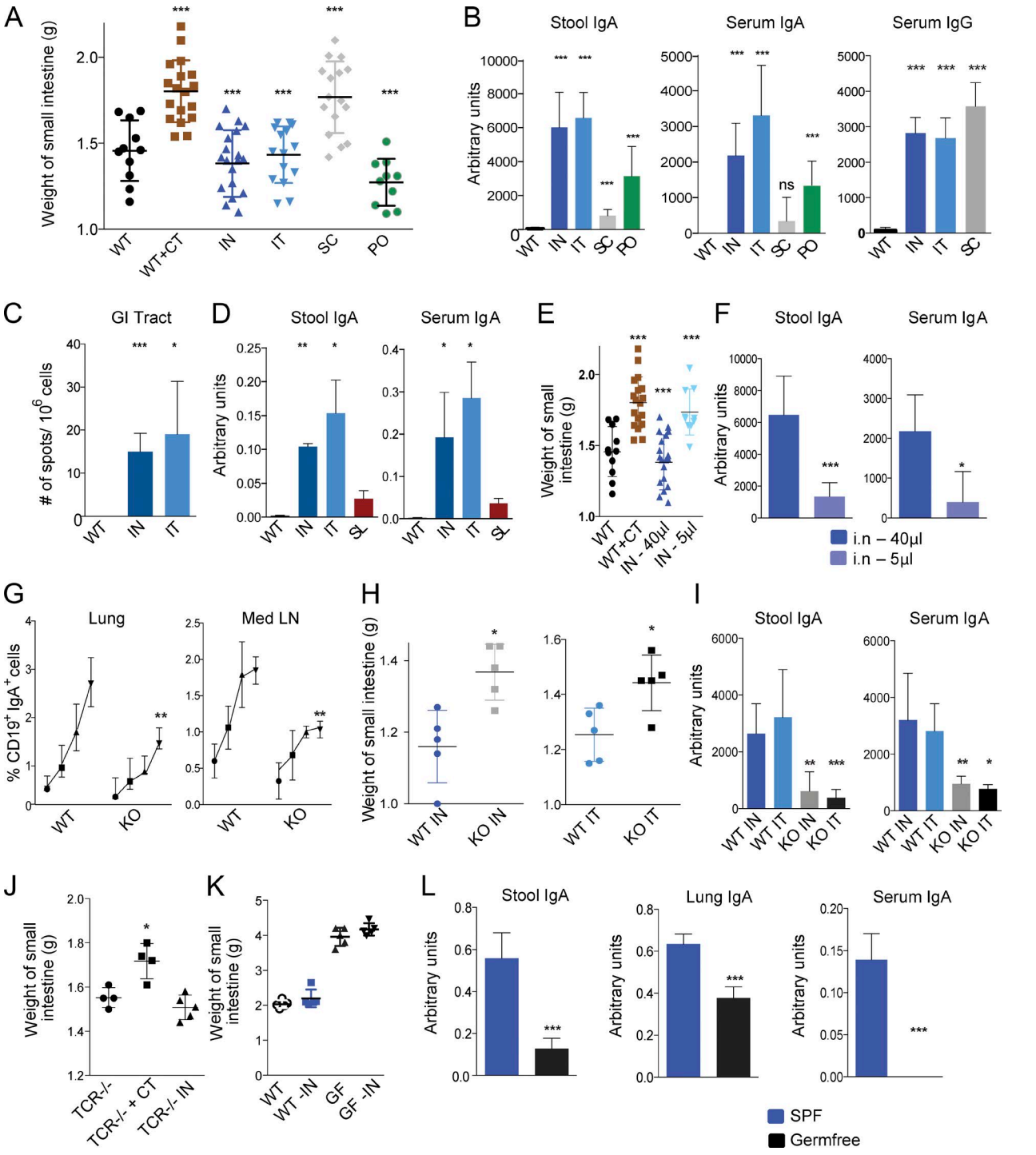

Figure 7. **Intranasal vaccination, targeting LDCs, confers protection against CT-induced diarrhea.** (A and B) CT-immunized mice (i.n., i.t., s.c., or p.o.) were challenged orally with CT 14 d after immunization. Cumulative data from at least three experiments is shown. Statistical comparisons to unimmunized (WT) mice are shown. (A) Quantification of the small intestinal weight. Horizontal bars, mean values; symbols, individual mice. (B) ELISA to quantify CT-specific IgA and IgG. (C) ELISPOT quantification of CT-specific IgA$^+$ cells in the GI tract after i.n. and i.t. immunization with CT. Unimmunized mice are represented as WT. Cumulative data from two experiments, five to six mice pooled per experiment. Statistical comparisons to unimmunized (WT) mice are shown. (D) ELISA quantification of IgA in the stool and serum from mice immunized i.n., i.t., or s.l. Cumulative data from 10 mice is shown. Statistical comparisons between i.n./i.t. and s.l immunized mice are shown. (E and F) Mice immunized i.n. with 2 µg of CT, delivered either in a volume of 40 µl or 5 µl were compared. Cumulative data from at least three experiments is shown. (E) Quantification of the small intestinal weight. Horizontal bars, mean values; symbols, individual mice. Statistical comparisons to unimmunized (WT) mice are shown. (F) ELISA quantification of CT-specific IgA in stool and serum.

TD versus TI Ig class switching comes from the influenza infection model wherein virus infection elicits a vigorous, $CD4^+$ T cell–dependent antibody response in WT mice (Bishop and Hostager, 2001). Although robust, TD IgG and IgM antibodies against influenza are well documented, perhaps the strongest evidence for a TI IgA response in the lung comes from an elegant study by Sangster et al. (2003). This group demonstrated that MHC II–deficient and CD40-deficient B cells produced little influenza virus-specific IgM and IgG, but generated a strong virus-specific IgA response with virus-neutralizing activity. They ascribed the TI IgA response to bystander help from T cells without being able to discern a clear source. Data presented in this study reconcile the observations of Sangster et al. (2003) and demonstrate that LDCs are able to induce IgA CSR, independent of T cell help, in a TGF-β and RA-dependent manner.

IgA plays important and diverse roles in mucosal homeostasis. In particular, opsonization and neutralization of pathogens and toxins results in immune exclusion, reducing antigenic load on the mucosal immune system. This is perhaps best demonstrated in protection models that use bacterial exotoxins (as used in the present study) or for pathogens that reside exclusively in the GI lumen. Several studies demonstrated a protective role for IgA at mucosal surfaces, wherein $IgA^{-/-}$mice show impaired clearance of luminal pathogens such as *Giardia muris* and *Giardia lamblia* (Langford et al., 2002), *Citrobacter rodentium* (Simmons et al., 2003), *Streptococcus pneumoniae* (Sun et al., 2004), and *Mycobacterium tuberculosis* (Rodríguez et al., 2005). In contrast, other studies have shown that protection against *Shigella flexneri* was similar in $IgA^{-/-}$ mice compared with WT mice (Way et al., 1999), implying a less critical role for IgA in mucosal defense. Yet another study showed $IgA^{-/-}$ mice were equally susceptible to primary infection with reovirus as WT mice, but showed increased susceptibility to reinfection (Silvey et al., 2001), again suggesting less of a role for IgA in defense against acute infection. However, an important and often overlooked caveat in such "negative" studies is that IgA deficiency in $IgA^{-/-}$ mice is accompanied by a compensatory increase in luminal IgM, perhaps as a result of reduced competition for the polymeric Ig (pIg) receptor (Harriman et al., 1999). Additionally, human data from patients with IgA deficiency clearly shows predisposition to sinopulmonary infections, colitis, and autoimmune diseases (Cunningham-Rundles, 2001; Jacob et al., 2008).

That said, the goal of our study was to examine the class switching function of LDCs in the context of nasal vaccination. To examine the physiological role of LDCs in IgA generation, we immunized *Batf3*$^{-/-}$ mice lacking $CD103^+$ DCs i.n. and i.t., and observed reduced levels of CT-specific IgA in the stool and serum of *Batf3*$^{-/-}$ mice compared with WT mice. Furthermore, the immunized *Batf3*$^{-/-}$ mice showed impaired protection against enteric challenge with CT. Combined, these data demonstrate that lung $CD103^+$ DCs are critical to the IgA response after CT immunization and are consistent with previous data that demonstrate a protective role of $CD103^+$ DCs in influenza infection (Helft et al., 2012).

Next, we looked for mechanistic factors within the lung APC subsets that determined their ability to induce IgA CSR and observed several important differences. First, the *TGF-β1* gene was up-regulated 19-fold in LDC $CD24^+$ and 2.5-fold in LDC $CD103^+$ compared with LMφ $CD64^+$. Second, *Aldh1a2*, encoding the vitamin A–metabolizing enzyme RALDH2, was up-regulated 10-fold in LDC $CD24^+$ and sixfold in LDC $CD103^+$ compared with LMφ $CD64^+$. Third, several B cell relevant genes were up-regulated in the LDC $CD24^+$ and LDC $CD103^+$ compared with LMφ $CD64^+$. Notable examples include NF-κb pathway-related genes that are associated with DC maturation (*Nfkb2*, *Chuk*, and *Ikbkb*), antigen presentation (*H2-ab1*, *H2-dma*, *H2-dmb1*, and *H2-dmb2*), *Icos* (Haimila et al., 2009), *Map3k14* (Tsuji et al., 2008), and *Ltβr* (Tsuji et al., 2008). Mutations in all of these genes have been associated with IgA deficiency.

Interestingly, LDC $CD24^+$, LDC $CD103^+$, and LMφ $CD64^+$ all expressed APRIL and BAFF, powerful IgA class-switching molecules (Litinskiy et al., 2002; He et al., 2007; Xu et al., 2007). In fact, whereas LMφ $CD64^+$ expressed the highest levels of *APRIL* and *BAFF* mRNA, the protein levels were equivalent between all the three APCs, likely reflecting the previously reported, extensive posttranscriptional and posttranslational (Stohl et al., 2004; Kawasaki et al., 2007) modification of these proteins. Thus, even though we did not observe IgA class switching by LMφ $CD64^+$ in vitro, given the high expression of APRIL and BAFF, it is possible that LMφ $CD64^+$ could cooperate with other cells in vivo and also participate in IgA class switching. Indeed, our data, in which addition of TGF-β and RA to LMφ $CD64^+$ B cell cultures resulted in robust IgA class switching, supports this possibility.

Investigation of the factors that modulate LDC ability to induce IgA CSR revealed an unexpected but significant

Statistical comparisons to between the two volumes of i.n. vaccine are shown. (G) Flow cytometric quantification of IgA^+ B cells in the lung and MedLN at steady state and after immunization with CT in WT or *Batf3*$^{-/-}$ (KO) mice. Cumulative data from two independent experiments is shown here with five mice per experiment. (H and I) CT-immunized WT and *Batf3*$^{-/-}$ (KO) mice were challenged orally with CT 14 d after immunization. (H) Quantification of the small intestinal weight after CT challenge. (I) ELISA to quantify CT-specific IgA in stool and serum. Horizontal bars, mean values; symbols, individual mice. Cumulative data from two independent experiments is shown. Statistical comparisons are made to immunized WT mice. (J) CT-immunized $TCR^{-/-}$ mice were challenged orally with CT 14 d after immunization. Small intestinal weight after CT challenge is demonstrated. (K and L) SPF or GF mice, immunized with CT were challenged orally after 14 d. Cumulative data from two experiments is shown. Statistical comparisons to SPF mice are shown. (K) Quantification of the small intestinal weight. Horizontal bars, mean values; symbols, individual mice. (L) ELISA quantification of CT-specific IgA in stool, lung, and serum. *, $P < 0.05$; **, $P < 0.01$; ***, $P < 0.001$.

role of the microbiota. Although the commensal microflora have a clear role in modulation of gut (Hill and Artis, 2010) and skin (Naik et al., 2012) immunity, their role in lung immune responses is less clear. Previous studies have linked changes within the microbiome with susceptibility to allergic airway disease (Noverr et al., 2005; Olszak et al., 2012; Russell et al., 2012, 2013) and influenza infection (Ichinohe et al., 2011). Here, we demonstrate that microbiota, acting through TLRs, condition LDCs to produce TGF-β and profoundly influence IgA production in the lung. Thus, the present study offers the first direct evidence linking microbial signals with the IgA class-switching function of LDCs. We are in the process of investigating whether IgA CSR function of LDCs is affected by the enteric microbiome or by oropharyngeal/pulmonary microbial communities.

Our next step was to investigate the migratory properties of LDC-induced B cells. Given that RA and TGF-β, shown here to influence IgA CSR, also induce gut-homing receptors, we hypothesized that B cells will up-regulate α4β7 and CCR9 upon culture with LDC. Contact-independent induction of gut-homing receptors was found to occur with the LDC $CD103^+$ and LDC $CD24^+$ but not LMφ $CD64^+$. In addition, after i.n. immunization, the frequency of $IgA^+\alpha4\beta7^+CCR9^+$ B cells in the lung progressively increased over 8 d. In vitro, the expression of α4β7 was seen on both IgA^+ and IgA^- B cells, which is in line with our observation that this was caused by secreted factors. These data are in agreement with previous results from our group, where we reported on the induction of gut-migratory T cells by LDC (Ruane et al., 2013) and support the concept of a common mucosal immune system originally proposed by Bienenstock et al. (1978).

In this study, we observed that LDC-conditioned B cells migrated to both the small intestines and the large intestines. Although we could identify markers known to be associated with small intestinal homing (CCR9; Mora et al., 2003), and panintestinal homing (α4β7; Villablanca et al., 2011), we did not detect the expression of GPR15, the only known large intestine–specific homing molecule (Kim et al., 2013) on LDC-induced B cells.

We undertook several lines of investigation to exclude inadvertent targeting of gut DCs by i.n. vaccination. First, we performed in vivo targeting experiments demonstrating that fluorescent antibodies delivered i.n. did not label gut-resident DCs. Second, we used the i.t. route of vaccine delivery to specifically target LDCs. Here, we found that the induction of intestinal IgA was comparable between i.t. and i.n. vaccination with CT and both routes of vaccine delivery, resulting in subsequent protection against GI challenge with CT. Finally, to exclude that serum IgA was being delivered via bile to the intestines, we found CT-specific IgA^+ cells in the GI tract using ELISPOT after i.n. vaccination with CT.

Because there is variance in the literature regarding the protective effect of i.n. vaccines, we have explored this further in our study. We hypothesized that i.n. vaccines that target LDCs may have a different effect than vaccines that do not. To test our hypothesis, we delivered the same dose of antigen in two different volumes: 5 and 40 µl. In vivo targeting experiments were done to show that at a volume of 5 µl, nasal DCs were targeted, and at 40 µl, nasal DCs, LDCs, and MedLN DCs were all targeted. Guided by these experiments, we immunized mice with CT (2 µg) delivered in a volume of either 5 or 40 µl. As shown in Fig. 7 (F and G), mice were protected against oral CT challenge if immunized with a volume of 40 µl but not 5 µl. These data, taken together with the data on induction of IgA by LDCs and the ability of LDCs to direct B cells to the GI tract, provide compelling evidence that for a nasally delivered vaccine LDCs should be targeted to induce GI-associated immune responses. This in turn argues for research into more efficacious and safer delivery systems to target LDCs by i.n. vaccines.

Finally, having demonstrated that the microbiota affect the production of IgA by LDC, we hypothesized that microbial signals will play an important role in i.n. vaccine-induced responses. In support of our hypothesis, we observed that GF mice, when immunized i.n., failed to generate specific IgA in the GI tract, unlike WT (SPF conditions) age-matched controls. Thus, efficacy of nasal vaccination, like systemic vaccination (Oh et al., 2014), may be significantly affected by microbial communities. A graphical summary of the major findings of our paper is provided in Fig. S4.

Some important caveats deserve mention here. We observed that CFSE dilution was milder in the LDC-B cell co-cultures compared with other DC–B cell cultures and hypothesized that this is a result of suppressive populations contained within LDCs. Because this was outside of the scope of the present study, we did not examine this question in further detail. We also detected interexperimental variance in the levels of IgA induced by LDCs that appeared to be physiological and related to the batch of mice used. Additionally, this paper does not address the contribution of lung-derived IgA^+ B cells to the total IgA pool in the gut. As such, significance of IgA originating in the lung to gut IgA responses at steady state remains to be determined.

In summary, the data generated in this study provide fundamental and novel insights on the generation of IgA by LDCs and help pave the way for better preventative and therapeutic strategies against mucosal diseases, both pulmonary and GI.

MATERIALS AND METHODS

Mice. C57BL/6 mice (B6) mice and were purchased from Taconic Farms or bred at The Rockefeller University or at Icahn School of Medicine at Mount Sinai. *Batf3*^{tm1Kmm}/J (*Batf3*$^{-/-}$) mice were purchased from The Jackson Laboratory Laboratories, $TCR^{-/-}$ mice were provided by the Cerutti laboratory. Mice were maintained in specific pathogen–free conditions. GF adult C57BL/6J mice were maintained in plastic gnotobiotic isolators at the Mount Sinai School of Medicine. $TRIF^{-/-}MyD88^{-/-}$ mice were provided by the Nussenzweig

laboratory (The Rockefeller University, New York, NY) and the Blander laboratory (Mount Sinai School of Medicine, New York, NY) and were used with the permission of S. Akira (Osaka University, Osaka, Japan). All experiments involving mice were performed in accordance with the guidelines of the animal care and use committee of Mount Sinai School of Medicine and The Rockefeller University.

Antibodies. The following reagents were from BD: anti-CD3 (500A2), anti-CD3 (145–2011), anti-CD103 (M290), anti-CD4 (RM4-5), biotin rat anti–mouse (C10-1), APC Streptavidin (554067), anti-CD64 (X54-5/7.1.1), and anti–Siglec-F (E50-2440). The following were from eBioscience: anti-MHCII (M5/114.15.2), anti-CCR9 (CW-1.2), anti-CD3 (500A2), and anti-CD4 (RM4-5). The following antibodies were from BioLegend: anti-CD45 (30-F11), anti-CD11b (M1/70), anti-CD19 (6D5), anti-CD103 (M290), anti–LPAM-1 (DATK32), anti-CD24 (M1/6a), anti-CCR9 (CW12), anti-CD64 (X54-51711), and anti-CD11c (N418). AQUA (L34957) was from obtained from Invitrogen and CFSE was purchased from Sigma-Aldrich.

Tissue harvesting and cell preparation. Mice were euthanized and blood was obtained from the experimental mice by cardiac puncture. Lung mononuclear cell isolation was performed as previously described (Vermaelen et al., 2001). In brief, after sacrificing the animals, the pulmonary circulation was perfused with saline to remove the intravascular pool of cells. Lungs were carefully separated from thymic and cardiovascular remnants and removed in toto. Organs were thoroughly minced using iridectomy scissors and incubated for 60 min in digestion medium containing collagenase D in a humidified incubator at 37°C and 5% CO_2. In the last 5 min, 10 mM EDTA was added. Tissue fragments were disrupted mechanically by pipetting and passed through a 70-μm cell strainer and mononuclear cells were washed twice in RPMI before using in subsequent experiments as described below.

The spleen and LN were harvested in RPMI media with 5% FCS, injected with collagenase D, and physically disrupted using a 25-gauge syringe. The cell suspension was placed in a humidified incubator at 37°C and 5% CO_2 for 25 min. In the last 5 min, 10 mM EDTA was added. Spleen but not LN samples went through subsequent ACK lysis, were washed twice and counted.

Intestinal lymphocytes were isolated and prepared as previously described (Mucida et al., 2007). In brief, small and large intestines were removed and placed in cold HBSS media containing 5% FCS. The intestines were carefully cleaned from the mesentery and flushed of fecal content. Intestines were opened longitudinally, and then cut into 1-cm pieces. The intestinal tissue was incubated with 1.3 mM EDTA (Cellgro) in HBSS at 37°C for 1 h. The supernatants containing intestinal epithelial cell (IEC) with some superficial villi cells, referred to as the IEC fraction, were not used in the present study. To isolate the lamina propria lymphocytes (LPL), the remaining intestinal tissue was minced and transferred to conical tubes. The minced pieces were resuspended in 20 ml of complete RPMI containing 0.125 mg/ml of collagenase (Sigma-Aldrich) and shaken at 200 rpm for 50 min at 37°C. The tissue suspension was collected and passed through a 70-μm cell strainer, and the cells were pelleted by centrifugation at 1,200 rpm. The cells were then resuspended and layered onto a 40/80% Percoll gradient, centrifuged, and collected, washed, and resuspended in complete RPMI media. These purified cells constituted the SILP or CLP lymphocyte population.

DC isolation. Single-cell suspensions were isolated from the murine lung, spleen, mesenteric, mediastinal, and skin draining LNs as described in the previous section. $CD11c^+$ cells were isolated as previously described (Ing et al., 2006) using CD11c magnetic beads (Miltenyi Biotec). In brief, the cells were washed in 1 ml of MACS buffer (Miltenyi Biotec), before 30 min incubation on ice with $CD11c^+$ beads. The cellular suspensions were washed twice in MACS buffer and passed through a magnetic column, and then $CD11c^+$ cells were isolated by positive selection, washed, resuspended in complete RPMI medium, and counted before co-culture with T cells as described below.

LDC subset isolation. Lung mononuclear cells were isolated as described in the previous subset. Using magnetic beads, $CD11c^+$ cells were enriched and sorted on FACSAria (BD) as Siglec-F^-MHC$II^+CD11c^{hi}CD103^+CD11b^-$ (LDC $CD103^+$), Siglec-F^-MHC $II^+CD11c^{hi}CD103^-CD11b^+$ $CD24^+CD64^-$ (LDC $CD24^+$), and Siglec-F^-MHC $II^+CD11c^{hi}CD103^-$ $CD11b^+$ $CD24^-CD64^+$ (LMφ $CD64^+$) subsets. To get sufficient numbers of DCs, LDCs were pooled from 5–10 mice per experiment, as indicated.

SpDC, SkDC, and MLN DC subset isolation. Mononuclear cells were isolated as described in Tissue harvesting and cell preparation. Using magnetic beads, $CD11c^+$ cells were enriched and sorted on FACSAria (BD) as $CD45^+MHCII^+CD11c^+$ cells.

In vitro DC/B cell co-cultures. The culture medium used for DC/B cell cultures was RPMI (Invitrogen) supplemented with 10% heat-inactivated FCS, 2 mM L-glutamine, 100 U/ml penicillin, 100 μg/ml streptomycin, and 5 mM β-mercaptoethanol (all from Sigma-Aldrich). B cells were negatively isolated using anti-CD43 MACs beads per manufacturer's instructions. In brief, this method relies on the fact that most leukocytes, except for resting mature B cells, express CD43 antigen. After magnetic bead isolation, cells were sorted and live $CD45^+$ $CD19^+$ IgM^+ B cells were obtained. These $CD43^{neg}CD19^+IgM^+$ B cells were added to round-bottom microtest wells at 10^5/well and mixed with isolated DCs at a DC/B cell ratio of 2:1. B cells were stimulated by adding 10 μg/ml Fab goat anti–mouse IgM (Jackson ImmonoResearch Laboratories) and 25 μg/ml anti-CD40 (BioLegend) After 4 d, the expression of IgA was investigated on B cells; addition-

ally, after 5 d, α4β7 and CCR9 expression on B cells was evaluated by FACS. For the RA inhibition assays, the DC/B cell co-culture were incubated with 3 μM of RAR-β antagonist LE540 (Wako) dissolved in DMSO at a stock concentration of 1 mM and added to cultures at final concentration of 3 μM. Additionally, to determine a dose response, LE540 was added to the DC/B cell cultures in concentrations of 2.5 μM, 250 nM, and 25 nM. For the TGF-β inhibition assay, 70–8.5 μg/ml of TGF-β pan-specific polyclonal antibody (R&D Systems) was added to the cultures. Anti–mouse IL-10 (eBioscience) and recombinant mouse TACI-Fc (BioLegend) at a final concentration of 10 μg/ml and 100 ng/ml, respectively, was added to the cultures on day 0 and 3.

Immunofluorescent microscopy. Immunofluorescent microscopy was performed according to standard protocols. In brief, sections were rehydrated in cold 1× DPBS for 5 min, fixed in 4% paraformaldehyde at room temperature for 5 min, permeabilized in 0.2% Triton at room temperature for 10 min. Next, sections were preincubated with blocking buffer (1× DPBS containing 1% BSA supplemented with 1% mouse and 1% rat serum) at room temperature for 1 h. To detect DCs, sections were incubated with CD11c conjugated with FITC at 2 μg/ml (clone N418; BioLegend), and April conjugated with PE at 0.5 μg/ml (clone A3D8; BioLegend) in blocking buffer. Nuclei were visualized by DAPI staining at 1 μg/ml (1 μg/ml DAPI in blocking buffer), and sections were mounted with ProLong Gold Antifade Mountant (Invitrogen). Images were taken using Zeiss Axioplan 2IE controlled by Zeiss AxioVision 4.6 software, and analyzed by ImageJ.

Competitive homing assay. $CD45.2^+CD43^{neg}CD19^+IgM^+$ B cells were cultured with flow sorted LDC (Siglec-F^-MHC $II^{hi}CD11c^{hi}$) or MLN DC ($CD45^+MHCII^+CD11c^{hi}$) or SpDC ($CD45^+MHCII^{hi}CD11c^{hi}$) in a ratio of 2:1 for 5 d. The respective B cells were labeled with 5 μM CFSE (Invitrogen) for 10 min at 37°C or 10 mM CMTMR (chloromethylbenzoyl-amino-tetramethylrhodamine; Life Technologies) for 20 min at 37°C. After washing twice with PBS, 5×10^5 CFSE-labeled B cells and 5×10^5 CMTMR-labeled B cells were injected via the retroorbital venous plexus into $CD45.1^+$ recipient mice. 18 h after transfer recipient mice were sacrificed and mononuclear cells isolated from the lung, spleen, SILP, and CLP. During FACS analysis, cells were gated on the congenic marker (e.g., CD45.2) and then on the specific B cell marker (e.g., CD19) and analyzed for the ratios between CMTMR- and CFSE-positive cells. The data are expressed as the HI, which is calculated as the ratio CFSE/CMTMR (or CMTMR/CFSE) in each tissue divided by the corresponding input ratio. $HI = CFSE_{tissue}/CMTMR_{tissue}:CFSE_{input}/CMTMR_{input}$.

Flow cytometric analyses, intracellular staining, and gating schema. Cells were isolated as described above. Before staining, cells were washed and resuspended in staining buffer containing 1× PBS, 2% BSA, 10 mM EDTA, and 0.01% NaN_3. To block nonspecific staining, the 2.4G2 anti-CD16/32 antibody was added. Antibodies for cell surface markers were added and cells were incubated for 25 min at 4°C. After the staining, the cells were washed twice and analyzed immediately or fixed in PBS containing 1% paraformaldehyde and 0.01% NaN_3 and analyzed later on an LSR II (BD) using multiparameter flow cytometry.

For intracellular cytokine staining, after surface staining, cells were resuspended in Fixation/Permeablization solution (BD Cytofix/Cytoperm kit; BD), and intracellular cytokine staining was performed according to the manufacturer's protocol. Flow cytometric data were analyzed with FlowJo software (Tree Star).

Microarray analyses. LDC and LMφ were obtained via flow sorting as described in the previous section. RNA was isolated using the TRIzol (Life Technologies) according to the manufacturer's instructions. Residual DNA was removed using the RNase-Free DNase Set (QIAGEN) on-column DNase treatment during RNeasy preparation. RNA was amplified by Illumina TotalPrep RNA Amplification kit and hybridized to the Expression BeadChip kit (Illumina). This chip was scanned using an Illumina HiScan. All datasets have been deposited at the National Center for Biotechnology Information Gene Expression Omnibus under accession no. GSE74969.

ELISA. Stool was collected from the respective mice and placed in 1 ml of protease inhibitor (Roche). Serum was isolated from the blood and stored at −20°C. ELISAs were performed by coating 96-well plates (Nunc) with 2.5 μg/ml CT, followed by blocking with PBS containing 2% BSA. After incubation of sera and stool, IgG and IgA were detected by using biotinylated antibodies, followed by streptavidin peroxidase (Jackson ImmunoResearch Laboratories). For detection of peroxidase activity, o-phenylenedi-amine dihydrochloride (Sigma-Aldrich) was added, and absorbance was measured at 450 nm.

ELISPOT. Plates were coated with 10 μg/ml CT (Sigma-Aldrich) overnight. After washing, plates were blocked with B cell media (RPMI containing 10% FBS [Gibco], 1% MEM NEAA [Gibco], 1% anti-anti [Gibco], and 0.1% 2-mercaptoethanol [Gibco]). Cells were plated in a concentration of $1–2 \times 10^6$ cells per well (GI) and cultured in B cell media for 24 h at 37°C, washed, and then isotype-specific antibody was detected using HRP-conjugated goat anti–mouse IgA secondary (Southern Biotech). Spots were developed using BD ELISPOT AEC substrate set (551951) according to manufacturer's protocol. Spots were quantified using a CTL-ImmunoSpot Analyzer and Software.

Microbiota transplantation. Protocol as previously described (Ridaura et al., 2013). In brief, cecal contents from WT mice

were suspended in PBS (2.5 ml per cecum) and were administered (0.2 ml per mouse) immediately to sterilely packed 7-wk-old C57BL/6 GF mice. Transplanted mice were maintained in sterile, unchanged cages for 4 wk.

Antibiotic treatment. Gender-matched wild-type mice were treated for 4 or 12 wk with Vancomycin (500 mg/l), neomycin (1 g/l), metronidazole (1 g/l), and ampicillin (1 g/l) in drinking water. Additionally, Splenda (artificial sweetener) was added (1 g/l) to improve palatability of water. Antibiotic-containing water was changed twice a week.

Immunization and CT challenge. Gender-matched WT mice, *Batf3*$^{-/-}$ mice, and TCR$^{-/-}$ mice (with appropriate controls) were immunized with 2 µg of CT from *Vibrio cholerae* (Sigma-Aldrich) in 5–40 µl of PBS i.n., i.t., or s.c. For s.l. vaccination, mice were immunized under the tongue in a volume of 7 µl. In other experiments, mice received 2 µg CT orally by gavage in 200 µl PBS. All animals were given food and water ad libitum. For the CT-induced diarrhea, 10 µg CT in 200 µl PBS was administered by oral gavage. 6 h before challenge, food and water were removed. 2 h after oral gavage, mice were sacrificed, and the weight of the small intestine was determined.

Fluorescent antigen uptake by LDCs. 8-12-wk-old WT mice were immunized i.n. with 50 µg of Ova-AF647 (Life Technologies) at two different volumes of either 5 or 40 µl. PBS-treated mice served as controls. After 24 h, LDCs were prepared as described previously and the uptake of OVA by the LDC subsets was examined.

Statistical analysis. Statistical significance was evaluated using a two-tailed Student's *t* test with a 95% confidence interval. Results are expressed as means ± SD. Analysis was performed with a Prism 4 program (GraphPad Software).

For microarray data analysis, images generated by the Illumina Hiscan were uploaded into GenomeStudio Software for primary data extraction and analysis. Spurious probes were filtered by translating the detection p-values into q-values (Storey and Tibshirani, 2003; Robinson et al., 2010) and removing any probe with maximum q-value across all samples ≥10%. Differential expression analyses of the resulting $\log_2$-transformed data were performed with SAM (Tusher et al., 2001) using the two-sample Wilcoxon or Mann-Whitney test statistic (other parameters were held to their default values). Genes assigned a false discovery rate less than 5% were considered differentially expressed. Enriched pathways and other gene sets, such as B cell activation and IgA CSR genes, were identified in the resultant lists of differentially expressed genes using the DAVID tool (Huang et al., 2009).

Primers. Table 1 shows the primers used for mouse gene amplification.

Table 1. **Primers used to amplify mouse gene products**

Gene	Primer
Cα GLT	Sense: 5′-CCAGGCTAGACAGAGGCAAG-3′ Antisense: 5′-CGGAAGGGAAGTAATCGTGA-3′
Aicda	Sense: 5′-GCCACCTTCGCAACAAGTCT-3′ Antisense: 5′-CCGGGCACAGTCATAGCAC-3′
Il10	Sense: 5′-GGTTGCCAAGCCTTATCGGA-3′ Antisense: 5′-ACCTGCTCCACTGCCTTGCT-3′
Il6	Sense: 5′-GGTACATCCTCGACGGCATCT-3′ Antisense: 5′-GTGCCTCTTTGCTGCTTTCAC-3′
Aldh1a2	Sense: 5′-ACCGTGTTCTCCAACGTCACTGAT-3′ Antisense: 5′-TGCATTGCGGAGGATACCATGAGA-3′
Baff	Sense: 5′-TGCTATGGGTCATGTCATCCA-3′ Antisense: 5′-GGCAGTGTTTTGGGCATATTC-3′
April	Sense: 5′-GCCTTCTGATCCTGACCGTGCC-3′ Antisense: 5′-AGTTTTGCGTTTGCCCGTGGA-3′
Integrin β8	Sense: 5′-CTGAAGAAATACCCCGTGGA-3′ Antisense: 5′-AGACTGTATGCCTCCCCAT-3′

Online supplemental material. Fig. S1 shows the gating strategy to identify and sort LDCs and MACs. Fig. S2 shows that LDCs, SpDCs, SkDCs, or MLN DCs were cultured with CD43^{neg}CD19^{+}IgM^{+} B cells in a DC/B cell ratio of 2:1 for 4 d in the presence of α-IgM and α-CD40 to stimulate B cells. Fig. S3 shows targeting of DCs with fluorescent antigens delivered i.n. Fig. S4 is a graphical summary of the paper. Online supplemental material is available at http://www.jem.org/cgi/content/full/jem.20150567/DC1.

ACKNOWLEDGMENTS

This work was supported by grants from the American Gastroenterology Association Elsevier Award (S. Mehandru), The Rockefeller University Clinical and Translation science award pilot project from National Institutes of Health/NCRR (5UL1RR024143-05; S. Mehandru) and R01 AI57653 (A. Cerutti).

The authors declare no competing financial interests.

Submitted: 30 March 2015

Accepted: 1 December 2015

REFERENCES

Annes, J.P., J.S. Munger, and D.B. Rifkin. 2003. Making sense of latent TGFβ activation. *J. Cell Sci.* 116:217–224. http://dx.doi.org/10.1242/jcs.00229

Barfod, K.K., M. Roggenbuck, L.H. Hansen, S. Schjørring, S.T. Larsen, S.J. Sørensen, and K.A. Krogfelt. 2013. The murine lung microbiome in relation to the intestinal and vaginal bacterial communities. *BMC Microbiol.* 13:303. http://dx.doi.org/10.1186/1471-2180-13-303

Bienenstock, J., M. McDermott, D. Befus, and M. O'Neill. 1978. A common mucosal immunologic system involving the bronchus, breast and bowel. *Adv. Exp. Med. Biol.* 107:53–59. http://dx.doi.org/10.1007/978-1-4684-3369-2_7

Bishop, G.A., and B.S. Hostager. 2001. B lymphocyte activation by contact-mediated interactions with T lymphocytes. *Curr. Opin. Immunol.* 13:278–285. http://dx.doi.org/10.1016/S0952-7915(00)00216-8

Bollinger, R.R., M.L. Everett, S.D. Wahl, Y.H. Lee, P.E. Orndorff, and W. Parker. 2006. Secretory IgA and mucin-mediated biofilm formation by environmental strains of *Escherichia coli*: role of type 1 pili. *Mol. Immunol.* 43:378–387. http://dx.doi.org/10.1016/j.molimm.2005.02.013

Casola, S., K.L. Otipoby, M. Alimzhanov, S. Humme, N. Uyttersprot, J.L. Kutok, M.C. Carroll, and K. Rajewsky. 2004. B cell receptor signal

strength determines B cell fate. *Nat. Immunol.* 5:317–327. http://dx.doi.org/10.1038/ni1036

Cerutti, A. 2008. The regulation of IgA class switching. *Nat. Rev. Immunol.* 8:421–434. http://dx.doi.org/10.1038/nri2322

Cerutti, A., and M. Rescigno. 2008. The biology of intestinal immunoglobulin A responses. *Immunity.* 28:740–750. http://dx.doi.org/10.1016/j.immuni.2008.05.001

Cerutti, A., X. Qiao, and B. He. 2005. Plasmacytoid dendritic cells and the regulation of immunoglobulin heavy chain class switching. *Immunol. Cell Biol.* 83:554–562. http://dx.doi.org/10.1111/j.1440-1711.2005.01389.x

Chaudhuri, J., and F.W. Alt. 2004. Class-switch recombination: interplay of transcription, DNA deamination and DNA repair. *Nat. Rev. Immunol.* 4:541–552. http://dx.doi.org/10.1038/nri1395

Choi, Y.S., and N. Baumgarth. 2008. Dual role for B-1a cells in immunity to influenza virus infection. *J. Exp. Med.* 205:3053–3064. http://dx.doi.org/10.1084/jem.20080979

Cunningham-Rundles, C. 2001. Physiology of IgA and IgA deficiency. *J. Clin. Immunol.* 21:303–309. http://dx.doi.org/10.1023/A:1012241117984

Dullaers, M., D. Li, Y. Xue, L. Ni, I. Gayet, R. Morita, H. Ueno, K.A. Palucka, J. Banchereau, and S. Oh. 2009. A T cell-dependent mechanism for the induction of human mucosal homing immunoglobulin A-secreting plasmablasts. *Immunity.* 30:120–129. http://dx.doi.org/10.1016/j.immuni.2008.11.008

Favre, L., F. Spertini, and B. Corthésy. 2005. Secretory IgA possesses intrinsic modulatory properties stimulating mucosal and systemic immune responses. *J. Immunol.* 175:2793–2800. http://dx.doi.org/10.4049/jimmunol.175.5.2793

Geissmann, F., P. Launay, B. Pasquier, Y. Lepelletier, M. Leborgne, A. Lehuen, N. Brousse, and R.C. Monteiro. 2001. A subset of human dendritic cells expresses IgA Fc receptor (CD89), which mediates internalization and activation upon cross-linking by IgA complexes. *J. Immunol.* 166:346–352. http://dx.doi.org/10.4049/jimmunol.166.1.346

Ginhoux, F., K. Liu, J. Helft, M. Bogunovic, M. Greter, D. Hashimoto, J. Price, N. Yin, J. Bromberg, S.A. Lira, et al. 2009. The origin and development of nonlymphoid tissue $CD103^+$ DCs. *J. Exp. Med.* 206:3115–3130. http://dx.doi.org/10.1084/jem.20091756

Guilliams, M., K. Crozat, S. Henri, S. Tamoutounour, P. Grenot, E. Devilard, B. de Bovis, L. Alexopoulou, M. Dalod, and B. Malissen. 2010. Skin-draining lymph nodes contain dermis-derived $CD103^-$ dendritic cells that constitutively produce retinoic acid and induce $Foxp3^+$ regulatory T cells. *Blood.* 115:1958–1968. http://dx.doi.org/10.1182/blood-2009-09-245274

Hahne, M., T. Kataoka, M. Schröter, K. Hofmann, M. Irmler, J.L. Bodmer, P. Schneider, T. Bornand, N. Holler, L.E. French, et al. 1998. APRIL, a new ligand of the tumor necrosis factor family, stimulates tumor cell growth. *J. Exp. Med.* 188:1185–1190. http://dx.doi.org/10.1084/jem.188.6.1185

Haimila, K., E. Einarsdottir, A. de Kauwe, L.L. Koskinen, Q. Pan-Hammarström, T. Kaartinen, K. Kurppa, F. Ziberna, T. Not, S. Vatta, et al. 2009. The shared CTLA4-ICOS risk locus in celiac disease, IgA deficiency and common variable immunodeficiency. *Genes Immun.* 10:151–161. http://dx.doi.org/10.1038/gene.2008.89

Harriman, G.R., M. Bogue, P. Rogers, M. Finegold, S. Pacheco, A. Bradley, Y. Zhang, and I.N. Mbawuike. 1999. Targeted deletion of the IgA constant region in mice leads to IgA deficiency with alterations in expression of other Ig isotypes. *J. Immunol.* 162:2521–2529.

He, B., W. Xu, P.A. Santini, A.D. Polydorides, A. Chiu, J. Estrella, M. Shan, A. Chadburn, V. Villanacci, A. Plebani, et al. 2007. Intestinal bacteria trigger T cell-independent immunoglobulin A(2) class switching by inducing epithelial-cell secretion of the cytokine APRIL. *Immunity.* 26:812–826. http://dx.doi.org/10.1016/j.immuni.2007.04.014

He, B., R. Santamaria, W. Xu, M. Cols, K. Chen, I. Puga, M. Shan, H. Xiong, J.B. Bussel, A. Chiu, et al. 2010. The transmembrane activator TACI triggers immunoglobulin class switching by activating B cells through the adaptor MyD88. *Nat. Immunol.* 11:836–845. http://dx.doi.org/10.1038/ni.1914

Helft, J., B. Manicassamy, P. Guermonprez, D. Hashimoto, A. Silvin, J. Agudo, B.D. Brown, M. Schmolke, J.C. Miller, M. Leboeuf, et al. 2012. Cross-presenting CD103+ dendritic cells are protected from influenza virus infection. *J. Clin. Invest.* 122:4037–4047. http://dx.doi.org/10.1172/JCI60659

Heng, T.S., and M.W. Painter. Immunological Genome Project Consortium. 2008. The Immunological Genome Project: networks of gene expression in immune cells. *Nat. Immunol.* 9:1091–1094. http://dx.doi.org/10.1038/ni1008-1091

Hildner, K., B.T. Edelson, W.E. Purtha, M. Diamond, H. Matsushita, M. Kohyama, B. Calderon, B.U. Schraml, E.R. Unanue, M.S. Diamond, et al. 2008. Batf3 deficiency reveals a critical role for $CD8\alpha^+$ dendritic cells in cytotoxic T cell immunity. *Science.* 322:1097–1100. http://dx.doi.org/10.1126/science.1164206

Hill, D.A., and D. Artis. 2010. Intestinal bacteria and the regulation of immune cell homeostasis. *Annu. Rev. Immunol.* 28:623–667. http://dx.doi.org/10.1146/annurev-immunol-030409-101330

Huang, W., B.T. Sherman, and R.A. Lempicki. 2009. Systematic and integrative analysis of large gene lists using DAVID bioinformatics resources. *Nat. Protoc.* 4:44–57. http://dx.doi.org/10.1038/nprot.2008.211

Huang, Y.J., E.S. Charlson, R.G. Collman, S. Colombini-Hatch, F.D. Martinez, and R.M. Senior. 2013. The role of the lung microbiome in health and disease. A National Heart, Lung, and Blood Institute workshop report. *Am. J. Respir. Crit. Care Med.* 187:1382–1387. http://dx.doi.org/10.1164/rccm.201303-0488WS

Ichinohe, T., I.K. Pang, Y. Kumamoto, D.R. Peaper, J.H. Ho, T.S. Murray, and A. Iwasaki. 2011. Microbiota regulates immune defense against respiratory tract influenza A virus infection. *Proc. Natl. Acad. Sci. USA.* 108:5354–5359. http://dx.doi.org/10.1073/pnas.1019378108

Ing, R., M. Segura, N. Thawani, M. Tam, and M.M. Stevenson. 2006. Interaction of mouse dendritic cells and malaria-infected erythrocytes: uptake, maturation, and antigen presentation. *J. Immunol.* 176:441–450. http://dx.doi.org/10.4049/jimmunol.176.1.441

Iwasaki, A., and B.L. Kelsall. 1999. Freshly isolated Peyer's patch, but not spleen, dendritic cells produce interleukin 10 and induce the differentiation of T helper type 2 cells. *J. Exp. Med.* 190:229–239. http://dx.doi.org/10.1084/jem.190.2.229

Jacob, C.M., A.C. Pastorino, K. Fahl, M. Carneiro-Sampaio, and R.C. Monteiro. 2008. Autoimmunity in IgA deficiency: revisiting the role of IgA as a silent housekeeper. *J. Clin. Immunol.* 28(S1, Suppl 1):S56–S61. http://dx.doi.org/10.1007/s10875-007-9163-2

Jacob, J., G. Kelsoe, K. Rajewsky, and U. Weiss. 1991. Intraclonal generation of antibody mutants in germinal centres. *Nature.* 354:389–392. http://dx.doi.org/10.1038/354389a0

Kawasaki, A., N. Tsuchiya, J. Ohashi, Y. Murakami, T. Fukazawa, M. Kusaoi, S. Morimoto, K. Matsuta, H. Hashimoto, Y. Takasaki, and K. Tokunaga. 2007. Role of APRIL (TNFSF13) polymorphisms in the susceptibility to systemic lupus erythematosus in Japanese. *Rheumatology (Oxford).* 46:776–782. http://dx.doi.org/10.1093/rheumatology/kem019

Kim, S.V., W.V. Xiang, C. Kwak, Y. Yang, X.W. Lin, M. Ota, U. Sarpel, D.B. Rifkin, R. Xu, and D.R. Littman. 2013. GPR15-mediated homing controls immune homeostasis in the large intestine mucosa. *Science.* 340:1456–1459. http://dx.doi.org/10.1126/science.1237013

Langford, T.D., M.P. Housley, M. Boes, J. Chen, M.F. Kagnoff, F.D. Gillin, and L. Eckmann. 2002. Central importance of immunoglobulin A in host defense against Giardia spp. *Infect. Immun.* 70:11–18. http://dx.doi.org/10.1128/IAI.70.1.11-18.2002

Langlet, C., S. Tamoutounour, S. Henri, H. Luche, L. Ardouin, C. Grégoire, B. Malissen, and M. Guilliams. 2012. CD64 expression distinguishes

monocyte-derived and conventional dendritic cells and reveals their distinct role during intramuscular immunization. *J. Immunol.* 188:1751–1760. http://dx.doi.org/10.4049/jimmunol.1102744

Litinskiy, M.B., B. Nardelli, D.M. Hilbert, B. He, A. Schaffer, P. Casali, and A. Cerutti. 2002. DCs induce CD40-independent immunoglobulin class switching through BLyS and APRIL. *Nat. Immunol.* 3:822–829. http://dx.doi.org/10.1038/ni829

Liu, Y.J., F. Malisan, O. de Bouteiller, C. Guret, S. Lebecque, J. Banchereau, F.C. Mills, E.E. Max, and H. Martinez-Valdez. 1996. Within germinal centers, isotype switching of immunoglobulin genes occurs after the onset of somatic mutation. *Immunity.* 4:241–250. http://dx.doi.org/10.1016/S1074-7613(00)80432-X

Macpherson, A.J., and T. Uhr. 2004. Induction of protective IgA by intestinal dendritic cells carrying commensal bacteria. *Science.* 303:1662–1665. http://dx.doi.org/10.1126/science.1091334

Macpherson, A.J., D. Gatto, E. Sainsbury, G.R. Harriman, H. Hengartner, and R.M. Zinkernagel. 2000. A primitive T cell-independent mechanism of intestinal mucosal IgA responses to commensal bacteria. *Science.* 288:2222–2226. http://dx.doi.org/10.1126/science.288.5474.2222

Mantis, N.J., M.C. Cheung, K.R. Chintalacharuvu, J. Rey, B. Corthésy, and M.R. Neutra. 2002. Selective adherence of IgA to murine Peyer's patch M cells: evidence for a novel IgA receptor. *J. Immunol.* 169:1844–1851. http://dx.doi.org/10.4049/jimmunol.169.4.1844

Martinoli, C., A. Chiavelli, and M. Rescigno. 2007. Entry route of *Salmonella* typhimurium directs the type of induced immune response. *Immunity.* 27:975–984. http://dx.doi.org/10.1016/j.immuni.2007.10.011

Mazanec, M.B., J.G. Nedrud, C.S. Kaetzel, and M.E. Lamm. 1993. A three-tiered view of the role of IgA in mucosal defense. *Immunol. Today.* 14:430–435. http://dx.doi.org/10.1016/0167-5699(93)90245-G

Moore, P.A., O. Belvedere, A. Orr, K. Pieri, D.W. LaFleur, P. Feng, D. Soppet, M. Charters, R. Gentz, D. Parmelee, et al. 1999. BLyS: member of the tumor necrosis factor family and B lymphocyte stimulator. *Science.* 285:260–263. http://dx.doi.org/10.1126/science.285.5425.260

Mora, J.R., M.R. Bono, N. Manjunath, W. Weninger, L.L. Cavanagh, M. Rosemblatt, and U.H. Von Andrian. 2003. Selective imprinting of gut-homing T cells by Peyer's patch dendritic cells. *Nature.* 424:88–93. http://dx.doi.org/10.1038/nature01726

Mora, J.R., M. Iwata, B. Eksteen, S.Y. Song, T. Junt, B. Senman, K.L. Otipoby, A. Yokota, H. Takeuchi, P. Ricciardi-Castagnoli, et al. 2006. Generation of gut-homing IgA-secreting B cells by intestinal dendritic cells. *Science.* 314:1157–1160. http://dx.doi.org/10.1126/science.1132742

Mucida, D., Y. Park, G. Kim, O. Turovskaya, I. Scott, M. Kronenberg, and H. Cheroutre. 2007. Reciprocal TH17 and regulatory T cell differentiation mediated by retinoic acid. *Science.* 317:256–260. http://dx.doi.org/10.1126/science.1145697

Muramatsu, M., K. Kinoshita, S. Fagarasan, S. Yamada, Y. Shinkai, and T. Honjo. 2000. Class switch recombination and hypermutation require activation-induced cytidine deaminase (AID), a potential RNA editing enzyme. *Cell.* 102:553–563. http://dx.doi.org/10.1016/S0092-8674(00)00078-7

Naik, S., N. Bouladoux, C. Wilhelm, M.J. Molloy, R. Salcedo, W. Kastenmuller, C. Deming, M. Quinones, L. Koo, S. Conlan, et al. 2012. Compartmentalized control of skin immunity by resident commensals. *Science.* 337:1115–1119. http://dx.doi.org/10.1126/science.1225152

Naito, T., T. Suda, K. Suzuki, Y. Nakamura, N. Inui, J. Sato, K. Chida, and H. Nakamura. 2008. Lung dendritic cells have a potent capability to induce production of immunoglobulin A. *Am. J. Respir. Cell Mol. Biol.* 38:161–167. http://dx.doi.org/10.1165/rcmb.2007-0237OC

Nardelli, B., O. Belvedere, V. Roschke, P.A. Moore, H.S. Olsen, T.S. Migone, S. Sosnovtseva, J.A. Carrell, P. Feng, J.G. Giri, and D.M. Hilbert. 2001. Synthesis and release of B-lymphocyte stimulator from myeloid cells. *Blood.* 97:198–204. http://dx.doi.org/10.1182/blood.V97.1.198

Nimmerjahn, F., and J.V. Ravetch. 2006. Fcgamma receptors: old friends and new family members. *Immunity.* 24:19–28. http://dx.doi.org/10.1016/j.immuni.2005.11.010

Nonoyama, S., D. Hollenbaugh, A. Aruffo, J.A. Ledbetter, and H.D. Ochs. 1993. B cell activation via CD40 is required for specific antibody production by antigen-stimulated human B cells. *J. Exp. Med.* 178:1097–1102. http://dx.doi.org/10.1084/jem.178.3.1097

Noverr, M.C., N.R. Falkowski, R.A. McDonald, A.N. McKenzie, and G.B. Huffnagle. 2005. Development of allergic airway disease in mice following antibiotic therapy and fungal microbiota increase: role of host genetics, antigen, and interleukin-13. *Infect. Immun.* 73:30–38. http://dx.doi.org/10.1128/IAI.73.1.30-38.2005

O'Neill, L.A., D. Golenbock, and A.G. Bowie. 2013. The history of Toll-like receptors - redefining innate immunity. *Nat. Rev. Immunol.* 13:453–460. http://dx.doi.org/10.1038/nri3446

Oh, J.Z., R. Ravindran, B. Chassaing, F.A. Carvalho, M.S. Maddur, M. Bower, P. Hakimpour, K.P. Gill, H.I. Nakaya, F. Yarovinsky, et al. 2014. TLR5-mediated sensing of gut microbiota is necessary for antibody responses to seasonal influenza vaccination. *Immunity.* 41:478–492. http://dx.doi.org/10.1016/j.immuni.2014.08.009

Olszak, T., D. An, S. Zeissig, M.P. Vera, J. Richter, A. Franke, J.N. Glickman, R. Siebert, R.M. Baron, D.L. Kasper, and R.S. Blumberg. 2012. Microbial exposure during early life has persistent effects on natural killer T cell function. *Science.* 336:489–493. http://dx.doi.org/10.1126/science.1219328

Peterson, D.A., N.P. McNulty, J.L. Guruge, and J.I. Gordon. 2007. IgA response to symbiotic bacteria as a mediator of gut homeostasis. *Cell Host Microbe.* 2:328–339. http://dx.doi.org/10.1016/j.chom.2007.09.013

Phalipon, A., and B. Corthésy. 2003. Novel functions of the polymeric Ig receptor: well beyond transport of immunoglobulins. *Trends Immunol.* 24:55–58. http://dx.doi.org/10.1016/S1471-4906(02)00031-5

Pilette, C., B. Detry, A. Guisset, J. Gabriels, and Y. Sibille. 2010. Induction of interleukin-10 expression through Fcα receptor in human monocytes and monocyte-derived dendritic cells: role of p38 MAPKinase. *Immunol. Cell Biol.* 88:486–493. http://dx.doi.org/10.1038/icb.2009.120

Quezada, S.A., L.Z. Jarvinen, E.F. Lind, and R.J. Noelle. 2004. CD40/CD154 interactions at the interface of tolerance and immunity. *Annu. Rev. Immunol.* 22:307–328. http://dx.doi.org/10.1146/annurev.immunol.22.012703.104533

Ridaura, V.K., J.J. Faith, F.E. Rey, J. Cheng, A.E. Duncan, A.L. Kau, N.W. Griffin, V. Lombard, B. Henrissat, J.R. Bain, et al. 2013. Gut microbiota from twins discordant for obesity modulate metabolism in mice. *Science.* 341:1241214. http://dx.doi.org/10.1126/science.1241214

Rimoldi, M., M. Chieppa, V. Salucci, F. Avogadri, A. Sonzogni, G.M. Sampietro, A. Nespoli, G. Viale, P. Allavena, and M. Rescigno. 2005. Intestinal immune homeostasis is regulated by the crosstalk between epithelial cells and dendritic cells. *Nat. Immunol.* 6:507–514. http://dx.doi.org/10.1038/ni1192

Robinson, M.D., D.J. McCarthy, and G.K. Smyth. 2010. edgeR: a Bioconductor package for differential expression analysis of digital gene expression data. *Bioinformatics.* 26:139–140. http://dx.doi.org/10.1093/bioinformatics/btp616

Rodríguez, A., A. Tjärnlund, J. Ivanji, M. Singh, I. García, A. Williams, P.D. Marsh, M. Troye-Blomberg, and C. Fernández. 2005. Role of IgA in the defense against respiratory infections IgA deficient mice exhibited increased susceptibility to intranasal infection with *Mycobacterium bovis* BCG. *Vaccine.* 23:2565–2572.

Ruane, D., L. Brane, B.S. Reis, C. Cheong, J. Poles, Y. Do, H. Zhu, K. Velinzon, J.H. Choi, N. Studt, et al. 2013. Lung dendritic cells induce migration of protective T cells to the gastrointestinal tract. *J. Exp. Med.* 210:1871–1888. http://dx.doi.org/10.1084/jem.20122762

Russell, S.L., M.J. Gold, M. Hartmann, B.P. Willing, L. Thorson, M. Wlodarska, N. Gill, M.R. Blanchet, W.W. Mohn, K.M. McNagny, and

B.B. Finlay. 2012. Early life antibiotic-driven changes in microbiota enhance susceptibility to allergic asthma. *EMBO Rep.* 13:440–447. http://dx.doi.org/10.1038/embor.2012.32

Russell, S.L., M.J. Gold, B.P. Willing, L. Thorson, K.M. McNagny, and B.B. Finlay. 2013. Perinatal antibiotic treatment affects murine microbiota, immune responses and allergic asthma. *Gut Microbes.* 4:158–164. http://dx.doi.org/10.4161/gmic.23567

Sangster, M.Y., J.M. Riberdy, M. Gonzalez, D.J. Topham, N. Baumgarth, and P.C. Doherty. 2003. An early $CD4^+$ T cell-dependent immunoglobulin A response to influenza infection in the absence of key cognate T–B interactions. *J. Exp. Med.* 198:1011–1021. http://dx.doi.org/10.1084/jem.20021745

Sato, A., M. Hashiguchi, E. Toda, A. Iwasaki, S. Hachimura, and S. Kaminogawa. 2003. $CD11b^+$ Peyer's patch dendritic cells secrete IL-6 and induce IgA secretion from naive B cells. *J. Immunol.* 171:3684–3690. http://dx.doi.org/10.4049/jimmunol.171.7.3684

Schlissel, M.S. 2003. Regulating antigen-receptor gene assembly. *Nat. Rev. Immunol.* 3:890–899. http://dx.doi.org/10.1038/nri1225

Schlitzer, A., N. McGovern, P. Teo, T. Zelante, K. Atarashi, D. Low, A.W. Ho, P. See, A. Shin, P.S. Wasan, et al. 2013. IRF4 transcription factor-dependent $CD11b^+$ dendritic cells in human and mouse control mucosal IL-17 cytokine responses. *Immunity.* 38:970–983. http://dx.doi.org/10.1016/j.immuni.2013.04.011

Schneider, P., F. MacKay, V. Steiner, K. Hofmann, J.L. Bodmer, N. Holler, C. Ambrose, P. Lawton, S. Bixler, H. Acha-Orbea, et al. 1999. BAFF, a novel ligand of the tumor necrosis factor family, stimulates B cell growth. *J. Exp. Med.* 189:1747–1756. http://dx.doi.org/10.1084/jem.189.11.1747

Sealy, R., S. Surman, J.L. Hurwitz, and C. Coleclough. 2003. Antibody response to influenza infection of mice: different patterns for glycoprotein and nucleocapsid antigens. *Immunology.* 108:431–439. http://dx.doi.org/10.1046/j.1365-2567.2003.01615.x

Seo, G.Y., Y.S. Jang, H.A. Kim, M.R. Lee, M.H. Park, S.R. Park, J.M. Lee, J. Choe, and P.H. Kim. 2013. Retinoic acid, acting as a highly specific IgA isotype switch factor, cooperates with TGF-β1 to enhance the overall IgA response. *J. Leukoc. Biol.* 94:325–335. http://dx.doi.org/10.1189/jlb.0313128

Silvey, K.J., A.B. Hutchings, M. Vajdy, M.M. Petzke, and M.R. Neutra. 2001. Role of immunoglobulin A in protection against reovirus entry into murine Peyer's patches. *J. Virol.* 75:10870–10879. http://dx.doi.org/10.1128/JVI.75.22.10870-10879.2001

Simmons, C.P., S. Clare, M. Ghaem-Maghami, T.K. Uren, J. Rankin, A. Huett, R. Goldin, D.J. Lewis, T.T. MacDonald, R.A. Strugnell, et al. 2003. Central role for B lymphocytes and $CD4^+$ T cells in immunity to infection by the attaching and effacing pathogen *Citrobacter rodentium*. *Infect. Immun.* 71:5077–5086. http://dx.doi.org/10.1128/IAI.71.9.5077-5086.2003

Spangler, B.D. 1992. Structure and function of cholera toxin and the related *Escherichia coli* heat-labile enterotoxin. *Microbiol. Rev.* 56:622–647.

Stavnezer, J. 1996. Antibody class switching. *Adv. Immunol.* 61:79–146. http://dx.doi.org/10.1016/S0065-2776(08)60866-4

Stavnezer, J., J.E. Guikema, and C.E. Schrader. 2008. Mechanism and regulation of class switch recombination. *Annu. Rev. Immunol.* 26:261–292. http://dx.doi.org/10.1146/annurev.immunol.26.021607.090248

Stohl, W., S. Metyas, S.M. Tan, G.S. Cheema, B. Oamar, V. Roschke, Y. Wu, K.P. Baker, and D.M. Hilbert. 2004. Inverse association between circulating APRIL levels and serological and clinical disease activity in patients with systemic lupus erythematosus. *Ann. Rheum. Dis.* 63:1096–1103. http://dx.doi.org/10.1136/ard.2003.018663

Storey, J.D., and R. Tibshirani. 2003. Statistical significance for genomewide studies. *Proc. Natl. Acad. Sci. USA.* 100:9440–9445. http://dx.doi.org/10.1073/pnas.1530509100

Sun, K., F.E. Johansen, L. Eckmann, and D.W. Metzger. 2004. An important role for polymeric Ig receptor-mediated transport of IgA in protection against *Streptococcus pneumoniae* nasopharyngeal carriage. *J. Immunol.* 173:4576–4581. http://dx.doi.org/10.4049/jimmunol.173.7.4576

Suzuki, Y., T. Suda, K. Furuhashi, K. Shibata, D. Hashimoto, N. Enomto, T. Fujisawa, Y. Nakamura, N. Inui, H. Nakamura, and K. Chida. 2012. Mouse CD11bhigh lung dendritic cells have more potent capability to induce IgA than $CD103^+$ lung dendritic cells in vitro. *Am. J. Respir. Cell Mol. Biol.* 46:773–780. http://dx.doi.org/10.1165/rcmb.2011-0329OC

Tezuka, H., Y. Abe, M. Iwata, H. Takeuchi, H. Ishikawa, M. Matsushita, T. Shiohara, S. Akira, and T. Ohteki. 2007. Regulation of IgA production by naturally occurring TNF/iNOS-producing dendritic cells. *Nature.* 448:929–933. http://dx.doi.org/10.1038/nature06033

Tokuhara, D., Y. Yuki, T. Nochi, T. Kodama, M. Mejima, S. Kurokawa, Y. Takahashi, M. Nanno, U. Nakanishi, F. Takaiwa, et al. 2010. Secretory IgA-mediated protection against V. cholerae and heat-labile enterotoxin-producing enterotoxigenic *Escherichia coli* by rice-based vaccine. *Proc. Natl. Acad. Sci. USA.* 107:8794–8799. http://dx.doi.org/10.1073/pnas.0914121107

Tsuji, M., K. Suzuki, H. Kitamura, M. Maruya, K. Kinoshita, I.I. Ivanov, K. Itoh, D.R. Littman, and S. Fagarasan. 2008. Requirement for lymphoid tissue-inducer cells in isolated follicle formation and T cell-independent immunoglobulin A generation in the gut. *Immunity.* 29:261–271. http://dx.doi.org/10.1016/j.immuni.2008.05.014

Tusher, V.G., R. Tibshirani, and G. Chu. 2001. Significance analysis of microarrays applied to the ionizing radiation response. *Proc. Natl. Acad. Sci. USA.* 98:5116–5121. http://dx.doi.org/10.1073/pnas.091062498

Vermaelen, K.Y., I. Carro-Muino, B.N. Lambrecht, and R.A. Pauwels. 2001. Specific migratory dendritic cells rapidly transport antigen from the airways to the thoracic lymph nodes. *J. Exp. Med.* 193:51–60. http://dx.doi.org/10.1084/jem.193.1.51

Villablanca, E.J., B. Cassani, U.H. von Andrian, and J.R. Mora. 2011. Blocking lymphocyte localization to the gastrointestinal mucosa as a therapeutic strategy for inflammatory bowel diseases. *Gastroenterology.* 140:1776–1784. http://dx.doi.org/10.1053/j.gastro.2011.02.015

Way, S.S., A.C. Borczuk, and M.B. Goldberg. 1999. Adaptive immune response to *Shigella flexneri* 2a cydC in immunocompetent mice and mice lacking immunoglobulin A. *Infect. Immun.* 67:2001–2004.

Wilkes, D.S., and J.C. Weissler. 1994. Alloantigen-induced immunoglobulin production in human lung: differential effects of accessory cell populations on IgG synthesis. *Am. J. Respir. Cell Mol. Biol.* 10:339–346. http://dx.doi.org/10.1165/ajrcmb.10.3.8117452

Wortis, H.H., M. Teutsch, M. Higer, J. Zheng, and D.C. Parker. 1995. B-cell activation by crosslinking of surface IgM or ligation of CD40 involves alternative signal pathways and results in different B-cell phenotypes. *Proc. Natl. Acad. Sci. USA.* 92:3348–3352. http://dx.doi.org/10.1073/pnas.92.8.3348

Xu, W., B. He, A. Chiu, A. Chadburn, M. Shan, M. Buldys, A. Ding, D.M. Knowles, P.A. Santini, and A. Cerutti. 2007. Epithelial cells trigger frontline immunoglobulin class switching through a pathway regulated by the inhibitor SLPI. *Nat. Immunol.* 8:294–303. http://dx.doi.org/10.1038/ni1434

Xu, W., P.A. Santini, A.J. Matthews, A. Chiu, A. Plebani, B. He, K. Chen, and A. Cerutti. 2008. Viral double-stranded RNA triggers Ig class switching by activating upper respiratory mucosa B cells through an innate TLR3 pathway involving BAFF. *J. Immunol.* 181:276–287. http://dx.doi.org/10.4049/jimmunol.181.1.276